RSPSE / Nuc Phys

2008

Next to PDF

Accelerator mass spectrometry of long-lived heavy radionuclides

L.K. Fifield*

Department of Nuclear Physics, Research School of Physical Sciences and Engineering, The Australian National University, Canberra, ACT 0200, Australia

Abstract

Accelerator mass spectrometry (AMS) is presently the most sensitive technique for the environmental measurement of radionuclides with half-lives greater than about 5000 years. Traditionally, it has been used principally for light elements, of which the most familiar example is ^{14}C. With some modifications, however, it may also be applied to elements as heavy as the actinides, and in particular to $^{239,240,244}Pu$ and ^{236}U. Here, the principles and methodology of heavy-element AMS are described, and the ways in which these have been implemented in various laboratories around the world are detailed. Although the emphasis is on plutonium and uranium, other isotopes such as ^{237}Np and $^{226,228}Ra$ are also considered. For completeness, the measurement of the long-lived fission products ^{99}Tc and ^{129}I by AMS is also discussed briefly. Actual or potential applications of the method in the areas of environmental science, biomedicine, and nuclear safeguards are reviewed.

1. Introduction

Anthropogenic α-particle emitting nuclides with half-lives that are long relative to the human life-span have been released into the environment by nuclear testing, nuclear accidents and reprocessing operations. Among the most significant are $^{239,240}Pu$, ^{236}U and ^{237}Np. Quantifying the releases, and tracing their subsequent dispersal has traditionally been the task of α-particle counting or, more recently, of thermal ionization or inductively coupled plasma (ICP) mass spectrometers. Although these are mature methodologies, each has its limitations. These limitations are largely surmounted by the relatively new technique of accelerator mass spectrometry (AMS).

For realistic counting times, α-particle counting is limited in sensitivity to ~50 μBq (O'Donnell et al., 1997). Counting times required for sensible results at this level are ~4 weeks. For ^{239}Pu, the limit corresponds to 20 fg. In addition, α-particle counting is unable to resolve the two most important plutonium isotopes, ^{239}Pu and ^{240}Pu, because their α-particle energies differ by only 11 keV in 5.25 MeV. Hence, information on the $^{240}Pu/^{239}Pu$ ratio, which is a useful indicator of the source of the plutonium, is not available.

* E-mail address: lkf103@rsphy1.anu.edu.au

RADIOACTIVITY IN THE ENVIRONMENT
VOLUME 11 ISSN 1569-4860/DOI: 10.1016/S1569-4860(07)11008-1

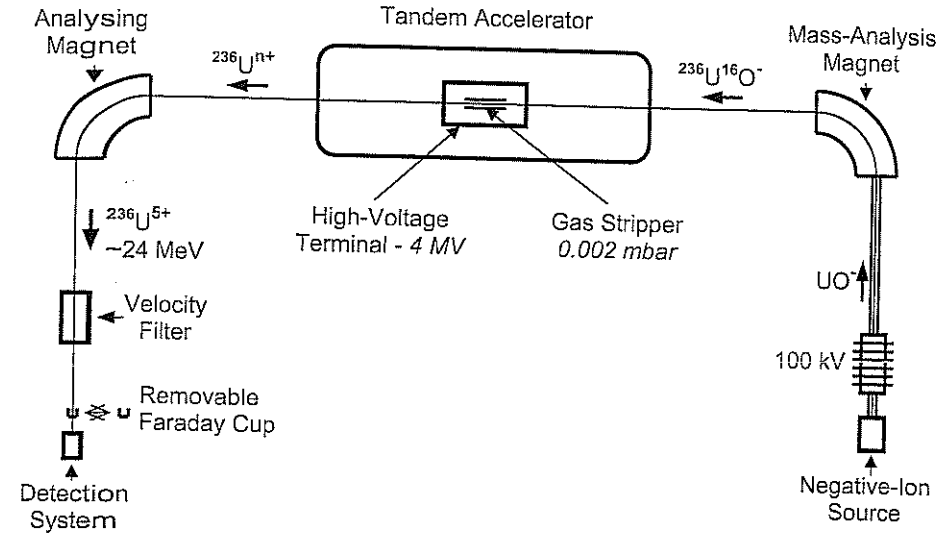

Fig. 1. Essential features of an AMS system for the measurement of ^{236}U.

Mass-spectrometric methods do give information on the $^{240}Pu/^{239}Pu$ ratio, and potentially have higher sensitivity than α-particle counting, with values as low as ~1 fg having been reported, but are sensitive to molecular interferences (Wyse et al., 2001). For example, ^{238}UH, $^{208}Pb^{31}P$, etc. could interfere with measurement of ^{239}Pu.

Accelerator mass spectrometry combines the high-sensitivity of the mass-spectrometric methods with a high level of discrimination against molecular interferences. The means of achieving this are described in detail below. Applications of the method are presented in subsequent sections. Although the principal emphasis of this chapter is on the α-particle emitting actinides, two particularly long-lived fission products, ^{99}Tc and ^{129}I, may also be measured by AMS with sensitivities that are considerably higher than competing techniques. These are also considered briefly below.

2. Principles of AMS as applied to heavy radionuclides

2.1. *Uranium-236*

It is convenient to introduce the concepts of the AMS method using ^{236}U as an illustrative example. Figure 1 shows the basic elements of an AMS system configured for ^{236}U. It consists essentially of two spectrometers separated by an accelerator that serves as a molecular dissociator. Its basic features are:

1. A low-energy mass spectrometer consisting of a *negative* ion source and a mass-analyzing magnet. The UO^- molecular ion is selected because the U^- atomic ion is produced only weakly by negative ion sources of the type employed for AMS.

2. Acceleration of the negative ions to the positive high-voltage terminal of a tandem electrostatic accelerator.
3. Dissociation of the molecules and removal of electrons to produce *positive* uranium ions.
4. Acceleration of the positive ions back to ground potential, followed by a second magnetic analysis that selects a single charge state with a well-defined energy.
5. An additional analysis by an electrostatic analyzer or velocity filter. The combination of magnetic and electrostatic analyses eliminates many of the potential sources of background.
6. A detection system, derived from the types of detectors used in basic nuclear physics research for detecting energetic charged particles, allows positive identification of each individual ^{236}U ion and the rejection of any remaining background ions.

AMS measures an isotope ratio, which would be $^{236}U/^{238}U$ in our illustrative example. The ^{236}U numerator is derived from the counting rate of ^{236}U ions in the detector. The ^{238}U denominator is derived by periodically switching the system to transmit ^{238}U ions through the full AMS system and measuring their flux as an electric current in a Faraday cup.

2.2. *Plutonium isotopes*

AMS of ^{236}U is more or less conventional in that the ^{236}U is measured by ion counting while the essentially "stable" isotope, ^{238}U, can be readily measured as an electric current. In the case of plutonium, there is no stable isotope. Hence, it is necessary to add a "spike" of a known amount of one of the long-lived isotopes, generally ^{242}Pu, to the sample in order to quantify the concentrations of the isotopes of interest, which are usually $^{239,240}Pu$ or ^{244}Pu. Both cost and radiological issues dictate that the amount of spike added is in the range 1–10 pg, in marked contrast to a typical uranium AMS sample that will contain a few milligrams of uranium. Consequently, both the isotopes of interest *and* the ^{242}Pu spike must be measured by ion counting (Fifield et al., 1997, 1996).

2.3. *Neptunium-237*

Neptunium-237 would be very similar to ^{239}Pu *if* pure ^{236}Np were readily available to use as a spike. Unfortunately, it is not, and measurements of ^{237}Np at both the ANU and Livermore have therefore been made relative to a ^{242}Pu spike (Brown et al., 2004; Fifield et al., 1997; Keith-Roach et al., 2001). This has two drawbacks. First, the ^{242}Pu must be added *after* the neptunium extraction chemistry, and hence does not compensate for any losses of yield in the extraction process. Secondly, the negative-ion formation probabilities of NpO^- and PuO^- are not the same. A value of 0.74 for the relative formation probability has been measured using a sample containing known amounts of ^{237}Np and ^{242}Pu (Keith-Roach et al., 2001). Both factors are additional sources of uncertainty. In principle, the first handicap may be overcome by using 2.4-day ^{239}Np as a chemical yield monitor that can be monitored via the 277 and 228 keV γ-rays emitted in its decay. The ^{239}Np may be milked from ^{243}Am retained on an ion-exchange column. Since the ^{243}Am stock contains some ^{241}Am, which is the parent of ^{237}Np, care must be taken to ensure that ^{237}Np has not had the opportunity to build up before the ^{239}Np is milked (Keith-Roach et al., 2001).

2.4. *Radium*

Both the ^{238}U and ^{232}Th decay series pass through radium isotopes. The ^{238}U series decays through ^{226}Ra, which is an α-particle emitter with a half life of 1600 years, long enough to make AMS detection an attractive alternative to α-decay counting. The ^{232}Th series decays through ^{228}Ra, which is a β-particle emitter with a half-life of only 5 years. Normally, AMS would not offer any advantages over decay counting for a lifetime as short as this. In order to identify ^{228}Ra uniquely by a decay-counting technique, however, it is necessary to detect the characteristic α-particles from the decay of its ^{228}Rn granddaughter, which has a half-life of 1.9 years. This necessitates a wait of 6 months or more for sufficient ^{228}Rn activity to grow in after separation of the radium from the sample. Hence a mass-spectrometric method such as AMS offers the benefit of faster turn-around time. Natural background isotopic concentrations typically found in soils are 1 pg/g for ^{226}Ra and 5 fg/g for ^{228}Ra, and hence the very high sensitivity of AMS offers significant advantages in terms of both sample size and a reduction in the complexity of sample preparation compared to α-particle spectroscopy.

The interest in radium stems from the need to monitor releases into the environment from uranium mining activities. If uranium is escaping into the environment, the spatial distribution of uranium will be more variable than that of thorium. Accordingly, measurements of the ^{226}Ra/^{228}Ra ratio may provide a probe with which to assess variations in the amount of uranium-process derived ^{226}Ra. Furthermore, for contaminated or rehabilitated areas where the ^{226}Ra/^{228}Ra ratio is anomalous, measurements of the transport of material away from the site via the ratio could provide information on the local erosion rate.

In contrast to plutonium or uranium, radium does not readily form the oxide molecular negative ion. Instead, the most prolific negative ion discovered to date is RaC_2^-. In order to prepare samples in a form that will produce a good yield of this negative ion, the radium is first separated with an anion exchange resin. Graphite powder is then added to the acid solution containing the radium and the solution evaporated to dryness before pressing into sample holders. The AMS method (Tims et al., 2004) closely follows that for plutonium.

AMS measures only the ^{228}Ra/^{226}Ra ratio. Since there are no other long-lived isotopes to use as a spike, an isotope dilution method must be employed in order to determine the concentrations. This involves the preparation of two samples, with and without the addition of a known amount of pure ^{226}Ra, and measuring the ^{228}Ra/^{226}Ra ratio for both.

2.5. *Iodine-129*

Iodine-129 is a prolific fission product, and has been released into the environment in considerable quantity by nuclear weapons testing, by nuclear accidents, Chernobyl and Three Mile Island in particular, and by controlled releases from nuclear-fuel reprocessing plants. A total of 2.4 tons of ^{129}I was released from the La Hague and Sellafield plants up to 1997, and this was increasing at the rate of ~300 kg/year (Raisbeck and Yiou, 1999). Because the discharges from both La Hague and Sellafield are carried into the North Atlantic by the Gulf Stream, ^{129}I is proving very useful as an oceanographic tracer in an area of the world's oceans that plays a vital role in the global thermohaline circulation (Gascard et al., 2004a, 2004b; Raisbeck and Yiou, 1999; Raisbeck et al., 1995; Yiou et al., 2004, 2002, 1994). AMS offers the advantages of very high sensitivity, and therefore small sample sizes. A liter of North

Atlantic water is sufficient for a measurement. Other applications have included *post facto* dosimetry of populations exposed to the Chernobyl accident, monitoring releases from nuclear facilities (Kilius et al., 1994; Rucklidge et al., 1994), and dating brines associated with oil fields, gas hydrates, or coalbed methane (Fehn et al., 2000, 2003; Fehn and Snyder, 2005; Moran et al., 1995; Snyder and Fehn, 2004, 2002; Snyder et al., 2003). In the Chernobyl application, long-lived ^{129}I has been used as a proxy for the much shorter-lived ^{131}I (Mironov et al., 2002). The latter is radiologically significant because it accumulates in the thyroid, but with a half-life of only 8 days, most of it had decayed away before it could be measured. Since the relative amounts of ^{131}I and ^{129}I in the Chernobyl fallout were well known, a later measurement of ^{129}I allows the exposure to ^{131}I to be determined.

Because the stable isobar, ^{129}Xe, does not form negative ions, ^{129}I may be measured almost equally well on small AMS systems operating with accelerating voltages as low as 0.5 MV as on larger systems operating at >5 MV (Kilius et al., 1990). Since iodine readily forms negative ions, $^{129}I^-$ is the negative ion of choice for injection into the accelerator. An electrostatic analyzer between ion source and mass-analyzing magnet is crucial in small-accelerator systems to eliminate the low-energy tail of the intense $^{127}I^-$ beam. In order to avoid interference from $M = 129$ molecular ions, charge state 3^+ or higher is selected for analysis after acceleration.

2.6. *Technetium-99*

Technetium-99 is also a prolific fission product, and has been released principally from the Sellafield plant. The largest releases took place between 1994 and 2003 following the commissioning of the Enhanced Actinide Recovery Plant, and averaged 150 kg/yr. Since 2003, a new recovery process has substantially reduced the amount released to the Irish Sea. Technetium-99 is a β-emitter with a half life of 212,000 years. Concentrations in seawater or seaweed have traditionally been measured using liquid-scintillation or gas-proportional counting of the β-decay after chemical extraction of the Tc to reduce other activities as much as possible, or by ICP-MS (Leonard et al., 2004; McCartney et al., 1999). Sensitivity of both the counting and mass-spectrometric techniques is at the level of pg of the isotope. The principal application has been in monitoring the dispersal of the Sellafield discharges, which are readily detectable along the Scandinavian coast across the North Sea. In a similar way to ^{129}I, it would be possible to use ^{99}Tc as an oceanographic tracer of North Atlantic circulation. Since ^{99}Tc was mostly sourced from Sellafield, whereas ^{129}I has been discharged from both La Hague and Sellafield, the two isotopes provide complementary information (Raisbeck and Yiou, 1999). Realization of the potential of ^{99}Tc, however, requires higher sensitivity than is available from radiometric or ICP-MS techniques.

AMS potentially offers higher sensitivity provided that the contribution from the ^{99}Ru isobar can be kept low. In practice this requires good chemistry to minimize any Ru in the sample to keep ^{99}Ru rates low in the detector, and a detector that can discriminate between ^{99}Tc and ^{99}Ru. Effective suppression of Ru can be achieved with a technetium-specific ion-exchange resin (Eichrom TEVA-Spec™), and this is now routinely employed for both decay-counting (to reduce ^{106}Ru) and ICP-MS (Leonard et al., 2004; McCartney et al., 1999). Discrimination between ^{99}Tc and ^{99}Ru requires an ionization detector that makes multiple measurements of the energy loss of the ions as they slow down in gas,

but this is only effective if the ion energy is at least 120 MeV (Bergquist et al., 2000; Fifield et al., 2000). Hence a large accelerator operating at >10 MV is required.

Sample preparation is again similar to that for plutonium. At the ANU, 10 pg of rhodium is added for normalization purposes after separation and purification of the Tc by ion exchange techniques, and the resulting mixture is dispersed in iron oxide. At Livermore, the Tc is dispersed in a niobium oxide matrix, and the ^{93}Nb beam current is used for normalization (Bergquist et al., 2000). The TcO^- negative ion is selected for analysis. Although the Tc^- ion is equally prolific, the choice of the oxide ion provides some suppression against Ru because the Ru^-/RuO^- ratio is greater than the Tc^-/TcO^- ratio (Fifield et al., 2000).

The AMS method developed at the ANU (Fifield et al., 2000) measures sequentially ^{103}Rh, ^{101}Ru, and ^{99}Tc in the 13^+ charge state at energies of ~200 MeV in order to determine the ^{99}Tc/^{103}Rh ratio. All three isotopes are measured by ion-counting in the ionization chamber. Measurement of ^{101}Ru allows subtraction of the ^{99}Ru contribution to the observed counting rate at mass-99 as an alternative to separating the ^{99}Tc and ^{99}Ru with the detector. This works well for samples where the bulk of the count rate is due to ^{99}Tc, but is insufficiently precise for samples with low ^{99}Tc concentrations. At Livermore, the ion energy is 125 MeV, and the ^{93}Nb beam current is measured in an off-axis Faraday cup after the analyzing magnet (Bergquist et al., 2000).

3. Advantages of AMS relative to conventional mass spectrometry

Both ^{236}U and plutonium isotopes have been measured by conventional mass spectrometry, using either thermal-ionization (TIMS) or inductively coupled plasma (ICP-MS) positive ion sources.

For uranium, outputs from TIMS and ICP ion sources are in the range of 10–100 pA of ^{238}U (~10^8–10^9 ions/s). Hence, at a ^{236}U/^{238}U ratio of 10^{-10}, which is at the upper end of the ratios found naturally in high grade uranium ores, the flux of ^{236}U ions would be only 0.01–0.1 s^{-1}. On the other hand, ratios can be 10^{-7} or higher in environments contaminated by nuclear accidents, reprocessing operations or depleted uranium projectiles, and ^{236}U fluxes are correspondingly higher. At these low counting rates it is necessary to use a secondary electron multiplier to count the ^{236}U ions. Background under the ^{236}U peak arises from the ^{235}UH molecule or other molecules of mass 236, and from the tail of the ^{238}U beam. The best reported UH^+/U^+ ratios from ICP sources using ultrasonic nebulizers and desolvators are $2–3 \times 10^{-6}$ (Ketterer et al., 2003). Hence the ^{235}UH contribution at mass-236 corresponds to a ^{235}UH/^{238}U ratio of 2×10^{-8}. Further, the low-energy tail of the intense ^{238}U beam is ~10^{-6} of the main peak (Ketterer et al., 2003). Variability in both the molecular and tail contributions limits the sensitivity of ICP-MS to ^{236}U/^{238}U ratios of ~10^{-7}. TIMS ion sources, on the other hand, produce much lower molecular beams, and a decelerating lens after magnetic analysis can reduce the ^{238}U tail to a negligible level. Background is then dominated by the dark noise of the electron multiplier and by scattered lighter-mass ions. Richter et al. (1999) report background counting rates of 10^{-2} s^{-1} and a sensitivity of 1×10^{-10} in the ^{236}U/^{238}U ratio.

In contrast to the lower currents available from TIMS and ICP sources, negative ion outputs from sputter sources are ~100 nA of $^{238}UO^-$, and even given typical transmission of 3%, still represent 2×10^{10} ^{238}U ions/s after acceleration. Hence, sufficient counts of ^{236}U can

be acquired to allow measurement of ratios as low as $\sim 10^{-12}$ provided that backgrounds are suitably low. At a ratio of 10^{-12}, ^{236}U ions would be detected at a rate of about 1 count per minute. The $^{235}U^{17}O$ or $^{238}U^{14}N$ molecular interferences, as well as other more exotic molecular interferences involving lighter elements such as $^{133}Cs^{107}Ag^{12}C$, are broken up in the stripper of the AMS system, and any backgrounds arising from the very small fraction of fragments that pass the subsequent analysis system are readily discriminated by the detection system at the high energies pertaining after acceleration.

For plutonium isotopes, abundance sensitivity is not a problem for conventional mass spectrometry due to the absence of a relatively intense beam of similar mass. Molecular interferences such as ^{238}UH, $^{208}Pb^{31}P$, etc. can still be a problem, however. These can be at least partially overcome with a high-resolution magnetic sector instrument, and sensitivities at the fg level have been reported for modern high-resolution ICP-MS systems (Wyse et al., 2001). Nevertheless, AMS offers advantages in terms of immunity to molecular interferences which might go unrecognized in a conventional system, and sensitivity can approach 0.1 fg (Brown et al., 2004; Fifield et al., 1997, 1996).

4. Advantages of AMS relative to α-spectrometry

Alpha-particle spectroscopy has been widely used for measuring plutonium concentrations, particularly for tracing releases from nuclear-fuel reprocessing facilities. The limit to its sensitivity is imposed by realistic counting times relative to the half-lives of the isotopes. Assuming a maximum counting time of one month, and a typical $^{240}Pu/^{239}Pu$ ratio of 20%, only 2×10^{-6} of the atoms would decay in this time. Since the (geometric) efficiency of detection is $\sim$0.3, fewer than one in a million of the Pu atoms in the sample will be detected. Realistically, the sensitivity limit is $\sim$50 μBq (O'Donnell et al., 1997) or 5×10^7 atoms. AMS is at least two orders of magnitude more sensitive.

The 20 Ma half-life of ^{236}U limits the utility of α-particle spectroscopy for this isotope. A realistic sensitivity limit of $\sim$50 μBq corresponds to 5×10^{10} atoms. Limited use of the technique has been made, for example, to search for the presence of depleted uranium resulting from the use of depleted uranium weaponry in Kosovo (Desideri et al., 2002).

An additional limitation of α-particle spectroscopy is that the measurement yields only the sum of the ^{240}Pu and ^{239}Pu activities, but not the $^{240}Pu/^{239}Pu$ ratio. Since the α-particle energies of the decays of the two isotopes differ by only 11 keV in 5.2 MeV, the two peaks are not resolved at typical detector energy resolutions of 25–40 keV. It is possible to deduce some information from centroid shifts, but since centroids are sensitive to details of sample deposition on the stainless steel discs employed, this method is imprecise at best.

5. Detailed description of AMS methodology

5.1. *Negative ion source*

The negative ion sources used in AMS are almost universally Cs sputter sources. These employ a focused beam of positive Cs ions to sputter material from the sample, and Cs vapor to

donate electrons to the sputtered atoms or molecules. The Cs beam is produced by surface ionization of some of the Cs vapor on a hot tantalum "ionizer". A voltage difference of 5–10 kV maintained between the ionizer and sample serves three functions: to focus the Cs ions on to the sample, to give the Cs ions sufficient energy to sputter effectively, and to extract the negative ions through a hole in the middle of the ionizer (Fifield, 1999). Typical sample masses are 1–10 mg, and the material is pressed into a hole in the sample holder that is typically 1 mm in diameter. The Cs beam is focused to a spot size on the sample of ~0.5 mm.

Samples for ^{236}U analyses are in the form of uranium oxide which is mixed with aluminum or silver powder to ensure electrical and thermal conduction. Atomic ratios of metal powder to uranium are in the range 1:1 to 4:1. In some applications, particularly in the safeguards area, only very small amounts of uranium are available. In these cases, the sample may be bulked with iron oxide (Hotchkis et al., 2000b; Marsden et al., 2001).

In the case of plutonium, macroscopic quantities of the element are not available, and it is necessary to disperse the atoms of plutonium in an iron oxide matrix. Again, aluminum or silver powder is mixed with the iron oxide to make the sample conducting.

Intensities of the molecular UO^- or PuO^- ions are two orders of magnitude greater than the atomic U^- or Pu^- ions, and hence the former are the ions of choice. Beam currents of ~100 nA of UO^- ions (6×10^{11} ions/s) may be extracted from a uranium oxide sample.

The question of efficiency of negative ion formation and extraction in these sources is taken up below under the discussion of sensitivity.

5.2. *Low energy mass analysis*

After extraction from the ion source, the negative ions are pre-accelerated to energies of 20–160 keV and then mass-analyzed by a 90° magnet. Relatively large magnets with radii between 30 and 100 cm are required to bend the very heavy ions. Further, the apertures at the object and image points of the magnet must be chosen to achieve a resolving power $M/\Delta M \sim 1000$, because it is important to prevent neighboring masses from entering the accelerator.

Switching between isotopes, ^{239}Pu, ^{240}Pu and ^{242}Pu for example, may be accomplished either by changing the magnetic field, or by changing the energy of the ions in the magnetic field while keeping the magnetic field fixed. The latter is achieved by applying a voltage to the vacuum box of the magnet, which clearly must be insulated for the purpose. At PuO^- energies of ~50 keV, the voltages required are ~0.4 and ~1.2 kV to switch from $^{239}PuO^-$ to $^{240}PuO^-$ and $^{242}PuO^-$, respectively.

5.3. *Acceleration and stripping*

Accelerators operating at 0.3 to 11 MV have been variously employed at different laboratories. Following mass analysis, the negative ions are accelerated to the high voltage terminal of a tandem accelerator where the molecular ions are dissociated and electrons removed from the resulting atoms to create multiply charged positive ions. This dissociation and stripping process generally takes place in low-pressure oxygen or argon gas, although very thin carbon foils are employed at the Munich laboratory. The now-positive ions, which are distributed across a range of charge states, are further accelerated back to ground potential. A single

charge state with a well-defined energy is then selected by another large magnet or electrostatic analyzer.

At those laboratories employing magnetic analysis, the accelerating voltage is invariably limited by the combination of the bending power of the magnet and the charge state probability distribution. At the ANU 14UD Pelletron accelerator, for example, the analyzing magnet can bend ions with ME/q^2 up to 220 MeV-amu. Here M is the mass of the ion in amu, E the energy in MeV, and q the charge on the ion in units of the electronic charge. In this case, the optimal compromise between transmission and stability is to analyze Pu^{5+} or U^{5+} ions. The maximum energy is then ~23 MeV which is achieved at an accelerating voltage of only ~4 MV (Fifield et al., 1996). This is well below the 11–14 MV at which the accelerator runs best, and requires that ~60% of the accelerator be shorted out. The considerations that determine this choice of charge state and hence of accelerating voltage are as follows:

- The stripping yield drops off rapidly with increasing charge state. For example, the yield in the 6^+ charge state is a factor of two less than in the 5^+, even allowing for the fact that it is possible to use a higher accelerating voltage of ~4.8 MV at the higher charge state.
- Although the stripping yield to the 4^+ charge state is higher than that of the 5^+, it would be necessary to operate the accelerator at ~3 MV in order that the ions could pass around the analyzing magnet. Because transmission through the accelerator is lower at this lower voltage, there is no net gain in using the lower charge state. There would, however, be advantages to using the lower charge states at smaller accelerators.

Equivalent considerations apply to the other laboratories where actinide AMS is practiced, but play out differently depending on the available hardware. Laboratory-specific details will be taken up later.

5.4. *Final analysis and detection*

Following the analyzing magnet, it is usual to have an additional analysis that involves an electric field. This may be either an electrostatic analyzer (ESA) or a velocity filter. The latter, also known as a Wien filter, employs crossed electric and magnetic fields to allow only ions with a definite velocity to pass undeflected. Since the analyzing magnet selects ions of constant ME/q^2, and an ESA or Wien filter selects ions of constant E/q or velocity (E/M) respectively, the combination of the two selects only ions which have the same M/q. An ESA with a 90° deflection angle has higher resolution than a Wien filter, but the latter has the advantage that it is simpler to align and can be turned off, to tune the beam for example.

Detectors fall into different categories, depending on the species to be detected. For Pu, backgrounds from uranium tend to be low (see the discussion of backgrounds below) because uranium concentrations in the sample can be reduced to very low levels with appropriate chemistry. If uranium background is negligible, then the detector has only to discriminate between Pu ions and lower-energy ions in lower charge states. To take a specific example, if Pu^{5+} ions are selected, the only background ions that reach the detector are 4^+, 3^+, 2^+ and 1^+ ions that have the same M/q as the plutonium. Since these have 4/5, 3/5, 2/5 and 1/5 of the plutonium energy, respectively, a simple energy measurement is usually all that is required to discriminate them from the Pu^{5+} ions. An ionization chamber is the detector of choice on the basis of robustness and adequate energy resolution, although silicon detectors have also been employed.

For ^{236}U, on the other hand, the sample contains unavoidably high levels of ^{238}U and ^{235}U, which are potent sources of background, even in an AMS system. The origins of these backgrounds will be discussed in more detail below, but it is sufficient to acknowledge at this point that even with a high-resolution ESA or Wien filter, there are inescapable backgrounds of ^{238}U and ^{235}U ions that limit the sensitivity of the ^{236}U/^{238}U ratio to $\sim 10^{-8}$ to 10^{-9} if they are not resolved from ^{236}U. An ionization chamber does not have sufficient energy resolution to separate the three uranium isotopes since the energies of the ^{238}U and ^{235}U ions differ by only -0.8% and 0.4%, respectively, from the ^{236}U ions. In order to achieve the required resolution, time-of-flight systems with a flight path of ~ 2 m have therefore been employed. An energy measurement is still required to separate the ^{236}U ions from the lower energy ions with the same M/q, since these have the same velocity and hence the same flight time as the ^{236}U ions.

An interesting recent development is the use of calorimetric low-temperature detectors, although these are still some way from routine application. These detectors measure the very small temperature changes produced by the heavy ion as it stops in a sapphire substrate. Temperature changes are manifested as changes in resistance of a thin-film superconducting aluminum strip thermometer operated close to its transition temperature of $T \approx 1.5$ K. Such detectors offer the advantage of considerably higher energy resolution compared to the more conventional ionization or silicon detectors. Kraft et al. (2004) reported relative energy resolutions, $\Delta E/E$, in the range 0.4–0.9% for 17 MeV uranium ions. This resolution approaches that, required to separate the different isotopes of uranium, and such detectors may in future be a viable alternative to time-of-flight detectors for ^{236}U measurements.

Each of these detection systems is described in more detail below.

5.4.1. *Ionization chambers*

Ionization chambers are simple and robust, and offer modest resolution that is generally sufficient to resolve lighter-mass ions of different charge q but approximately the same mass/charge ratio (m/q) as the ions of interest. Only a total energy measurement is required.

At the ANU, a resolution $\Delta E/E = 3\%$ is achieved for 23 MeV plutonium ions. Propane is employed as the detector gas at a pressure of 55 Torr, and the ions pass into the detector through a 0.7 μm mylar window with a diameter of 13 mm, losing ~ 3 MeV or 13% of their energy in the process. Typical energy spectra are shown in Figure 2. The origin of the non-plutonium peaks in these spectra are considered in the discussion of backgrounds below. This detector is also used for ^{237}Np and ^{226,228}Ra.

At the other extreme, an ionization detector is also used by the Zurich group (Wacker et al., 2005), but to detect plutonium ions with an energy of only 1.2 MeV. A silicon nitride membrane with a thickness of 40 nm and an area of 3×3 mm^2 retains the isobutane gas at a typical pressure of 15 mbar. The realization that these ultra-thin silicon nitride membranes made excellent detector windows was crucial to this application since 1.2 MeV plutonium ions would stop in the thinnest available mylar (0.5 μm) but lose only 25% of their energy in the silicon nitride. Considerable attention has also been paid to reducing the electronic noise in this detector by minimizing capacitance and using cooled FET pre-amplifiers (Suter et al., 2007). The noise contribution to the resolution is equivalent to only 12 keV in ion energy. Typical spectra which contrast the performance of a silicon detector with a low-noise ion chamber with two different thicknesses of silicon nitride window are shown in Figure 3

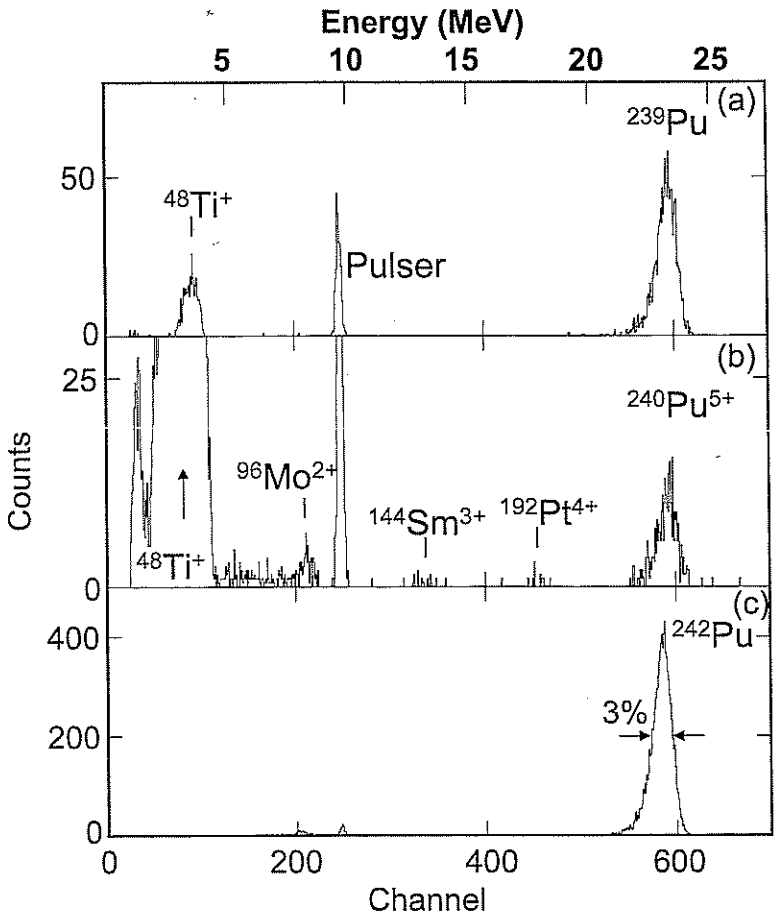

Fig. 2. Energy spectra from the ionization chamber for (a) ^{239}Pu, (b) ^{240}Pu, and (c) ^{242}Pu from a "typical" environmental sample where the Pu was derived from global fallout. A spike of 4 pg of ^{242}Pu was added to the sample for normalization purposes. Acquisition times were 2, 3, and 1 min, respectively. The pulser served to monitor dead-time in the electronics and data acquisition system. Note that the ^{240}Pu spectrum shows peaks at lower energy that arise from fragments of molecules that were dissociated in the gas stripper and subsequently passed the high-energy analysis. These are identified by atomic species, isotope and charge state. Events that fall between the intense ^{48}Ti peak and the ^{96}Mo peak are due to pile-up of two ^{48}Ti ions that arrive within the resolving time of the detector electronics. Careful inspection of the Pu peaks reveals the expected small centroid shifts from one isotope to the next.

(Wacker et al., 2005). Resolution of the ion chamber with a 40 nm silicon nitride window is ~20% of the signal height. Note, however, that the magnitude of the signal does not represent the full 1.2 MeV of the incoming ions but is reduced by the twin factors of energy loss in the window and pulse height defect. Plutonium ions at these low energies lose a substantial fraction of their energy in the gas, not in collisions with electrons to produce ionization, but by so-called "nuclear scattering", which is actually an ion-atom scattering process in which the moving plutonium ion transfers energy to a gas atom as a whole. According to the program

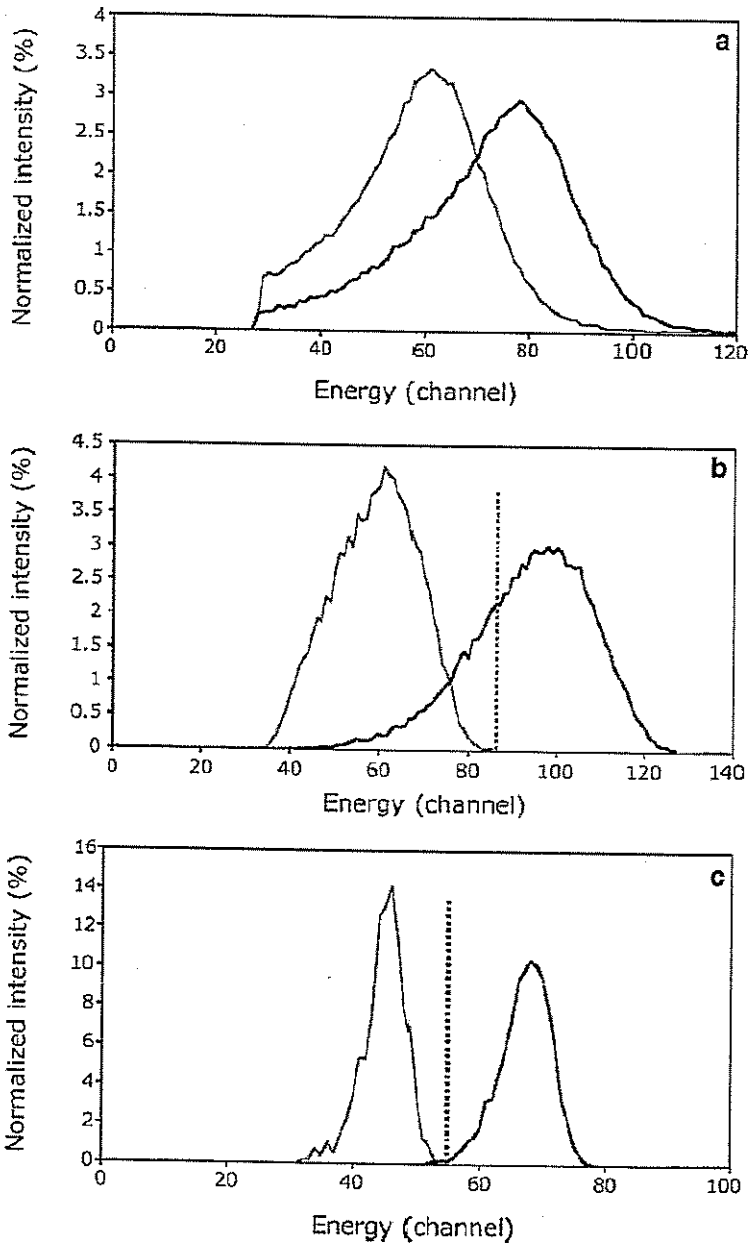

Fig. 3. The spectra obtained from (a) a surface barrier detector, (b) a gas ionization detector with a 100 nm Si–N window, and (c) a gas ionization detector with a 40 nm Si–N window are shown, for 1.2 MeV $^{240}Pu^{3+}$ (black line) or 0.8 MeV $^{160}Dy^{2+}$ (gray line) ions. The dotted line marks the low level discriminator to cut off virtually all 2^+ ions. [From Wacker et al. (2005).]

TRIM of Ziegler and Biersack (2003), only about 30% of the plutonium energy is transferred directly to ionization. Fortunately, the recoiling gas atoms also create ionization as they slow down in turn, with the net result that ~70% of the available energy ultimately appears as ionization. Given that the ions lose ~0.4 MeV in the silicon nitride window, and that ~70% of what is left is converted to ionization, the signal height is equivalent to the deposition of only about half of the original 1.2 MeV in the detector gas.

5.4.2. *Time-of-flight systems*

Time-of-flight systems (TOF) for AMS consist of "start" and "stop" detectors typically separated by 2 m, and also incorporate a measurement of the ion's energy. Start detectors must transmit the ions, and hence are all based on the collection of electrons liberated from a thin carbon foil as the ions pass through it. The electrons are accelerated to typically 1 keV, and transported isochronously to a micro-channel plate (MCP) assembly. MCPs may be operated at very high gain of $\sim 10^7$, and produce very fast output pulses with rise times of ~1 ns that are ideal for fast-timing applications. In order to minimize losses of ions due to scattering, the carbon foils should be as thin as possible. Diamond-like carbon foils as thin as 0.5 $\mu g/cm^2$ (Liechtenstein et al., 2004) are now widely used, although they have the disadvantage that they must be supported on a copper mesh with a transparency of only 75%. Isochronous transport of the electrons has been accomplished in one of two ways:

(i) Orienting the carbon foil normal to the incoming ions, and reflecting the electrons through 90° with an electrostatic mirror to transport them to the MCP which is out of the ion path.
(ii) Orienting the carbon foil at 45° to the incoming ions. The MCP can then be mounted parallel to the foil but out of the ion path, and views the upstream side of the foil so that it does not see scattered ions. This system has the advantage that it requires two fewer grids than the mirror device, and one less high-voltage power supply, but has the disadvantage that there is a geometric contribution to the timing resolution due to the 45° tilt of the foil. For example, if the beam has a full width at half maximum (fwhm) of 2 mm at the foil, there will be a variation of 2 mm in flight path. This translates into a contribution of 460 ps to the resolution of the TOF system for 23 MeV uranium ions.

The stop detector may be either a silicon detector, in which case it also provides the measurement of the ion's energy, or another MCP detector. In order to collect as many as possible of the ions that passed through the start detector, active areas of at least 25 mm in diameter are advantageous. Because of the large area, only the mirror design of MCP detector is suitable. If the MCP option is adopted, then it must be followed by either an ionization chamber or silicon detector to provide the energy information.

Although intrinsic resolutions of 0.3–0.4 ns have been reported for such TOF systems (Steier et al., 2002), in practical situations the observed resolution is generally about 1 ns. As can be seen from Table 1, this resolution is sufficient to separate ^{236}U from ^{235}U and ^{238}U ions of the same magnetic rigidity provided that count rates of the latter are low. This is illustrated by Figure 4, which shows a two-dimensional plot of energy vs TOF and the one-dimensional projection on to the TOF axis for a sample with $^{236}U/^{238}U = 6 \times 10^{-11}$.

A drawback of a TOF system is that its efficiency is typically only 30–50% due both to losses on the multiple grids and foil-supporting meshes of the start and stop detectors, and to losses due to beam divergence and scattering in the foil of the start detector.

Table 1
Flight times over a 2 m flight path for 5^+ uranium ions of different masses but the same magnetic rigidity. Energies are typical of those used at the ANU

Ion	Energy (MeV)	Flight time, T (ns)	ΔT (ns)
^{235}U	23.995	518.3	−2.2
^{236}U	23.893	520.5	
^{238}U	23.692	525.0	4.4

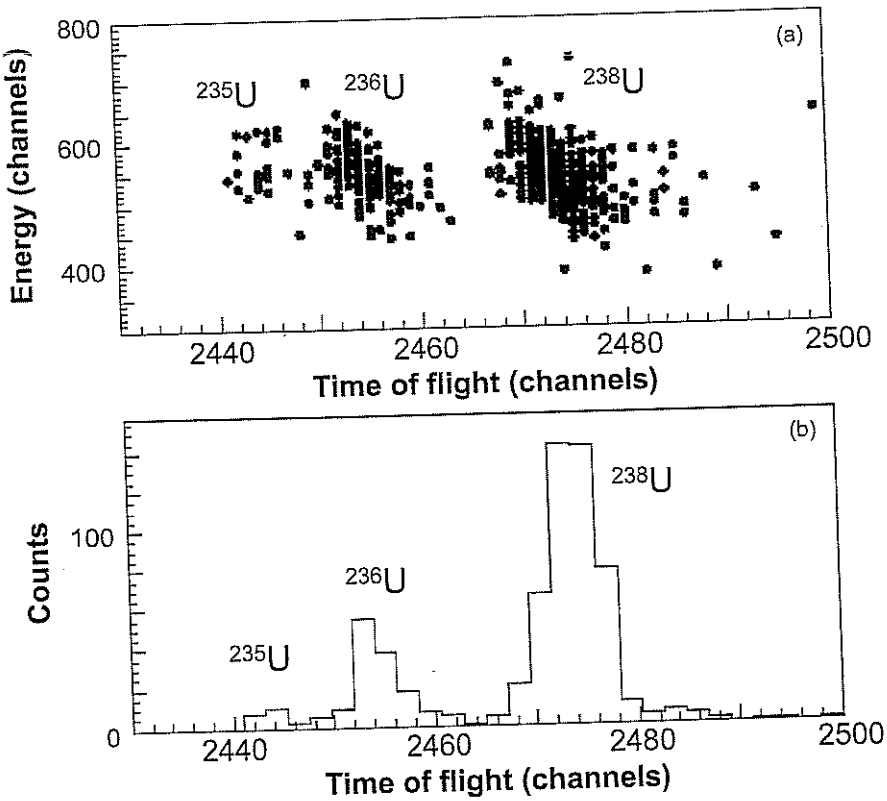

Fig. 4. (a) Two-dimensional spectrum of energy deposited in the Si detector vs TOF for a uranium ore sample with a $^{236}U/^{238}U$ ratio of 6×10^{-11}. (b) One-dimensional projection of (a) on to the TOF axis.

6. Implementation at various laboratories

6.1. *ANU*

At the ANU, the accelerating voltage of ~4 MV and the choice of the 5^+ charge state are dictated by the maximum mass–energy product (220 MeV-amu) of the 90° analyzing magnet. A Wien filter is employed to remove backgrounds which have the same ME/q^2 as the ions

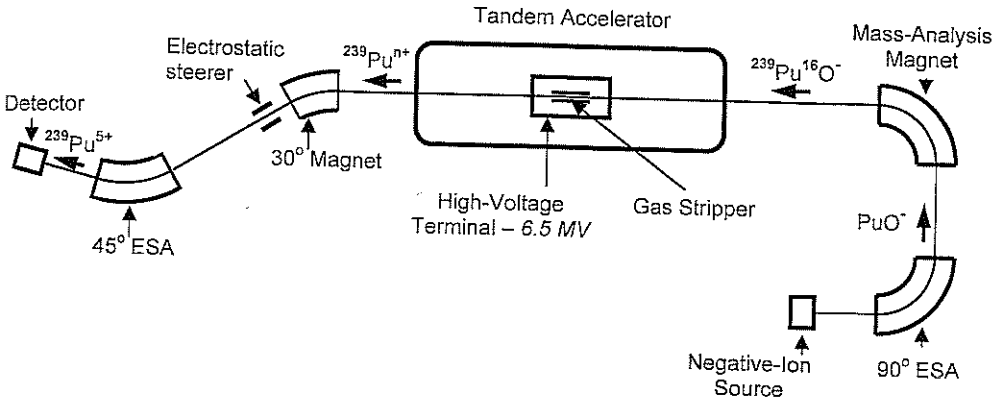

Fig. 5. AMS system for the measurement of actinides at Lawrence Livermore National Laboratory. [After Brown et al. (2004).]

of interest but different velocities. Switching between different isotopes is accomplished by changing

(i) the field in the injection magnet,
(ii) the terminal voltage of the accelerator, and
(iii) the electric field of the Wien filter.

Switching times in this slow-cycling procedure are 15 s. For plutonium, measurement times are generally 1 min at ^{242}Pu, 3 min at ^{240}Pu and 2 min at ^{239}Pu. This sequence is repeated as many times as necessary, with 3 loops being typical. For ^{236}U, each loop consists of integration of the ^{238}U beam current for 10 s, and counting of ^{236}U ions for 5 min.

Detection systems are an ionization chamber for ^{239}Pu, ^{237}Np or ^{226,228}Ra, and a TOF system for ^{236}U. Only the total energy signal from the ionization detector is recorded, since it is necessary to distinguish only between the 5^+ Pu ions with energy of ~23 MeV, and ions in lower charge states with 4/5, 3/5, 2/5 and 1/5 of this energy.

6.2. *Lawrence Livermore National Laboratory*

At Livermore, an analyzing magnet with a deflection angle of only 30° followed by a 45° ESA allows the use of a higher terminal voltage of 6.5 MV. This arrangement is depicted in Figure 5. Again, gas-stripping is employed and the 5^+ charge state is selected. The detection system for plutonium, ^{237}Np, and ^{236}U is a two-anode longitudinal-field ion chamber (Brown et al., 2004; McAninch et al., 2000).

Switching between isotopes is accomplished with a fast-switching system. Different voltages are applied to the vacuum box of the injection magnet in order to inject the various isotopes into the accelerator. An electrostatic steerer after the 30° analyzing magnet directs the different isotopes through the image slits of the magnet and into the ESA. The all-electric switching can be fast, ~10 μs. Measurement times are 0.1 s for ^{242}Pu and 0.4 s for ^{239}Pu and ^{240}Pu. Cycling between the ^{242}Pu–^{239}Pu pair continues for 10 s before changing to the ^{242}Pu–^{240}Pu pair for the next 10 s.

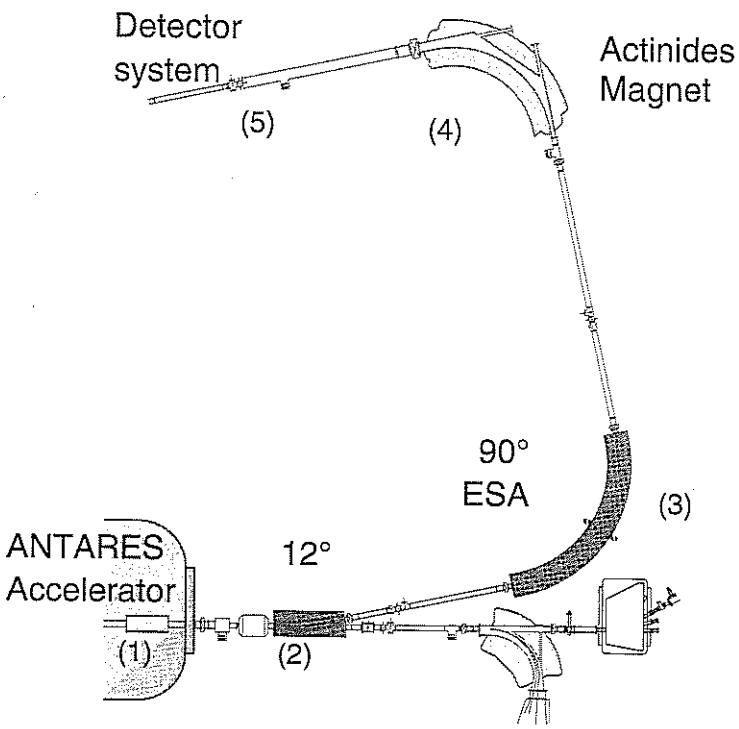

Fig. 6. High-energy actinide beam-line at the ANTARES facility at the Australian Nuclear Science and Technology Organisation (ANSTO). [Reprinted with permission from Hotchkis et al. (2000a).]

6.3. *ANSTO*

The operating conditions at ANSTO are essentially the same as at the ANU, i.e. the accelerating voltage is 4 MV and the 5^+ charge state is selected. There the similarities end, however.

A heavy-element beam-line consisting of a high-resolution, 2.5 m radius, 90° ESA followed by a large (2.0 m radius) 90° magnet (Figure 6) has been constructed to analyze the ~24 MeV heavy ions after acceleration (Hotchkis et al., 2000a, 2000b). The advantage of having the magnet as the final element in the system is that, for a given charge state, it disperses in mass following the E/q selection of the ESA. Hence the focal plane of the magnet can be instrumented at specific locations with various detection systems tailored to the intensity of the isotopes to be measured. An ionization chamber is employed for Pu measurements, which is preceded by a TOF system, comprised of two micro-channel plate detectors for ^{236}U measurements. The more intense ^{238}U, ^{235}U or ^{234}U beams can be measured by either Faraday cups or an electron multiplier, as shown in Figure 7.

6.4. *VERA*

Despite the lower terminal voltage of 3 MV of the VERA accelerator, the 5^+ charge state is selected because this is the minimum charge that the 90° analyzing magnet can bend (Steier

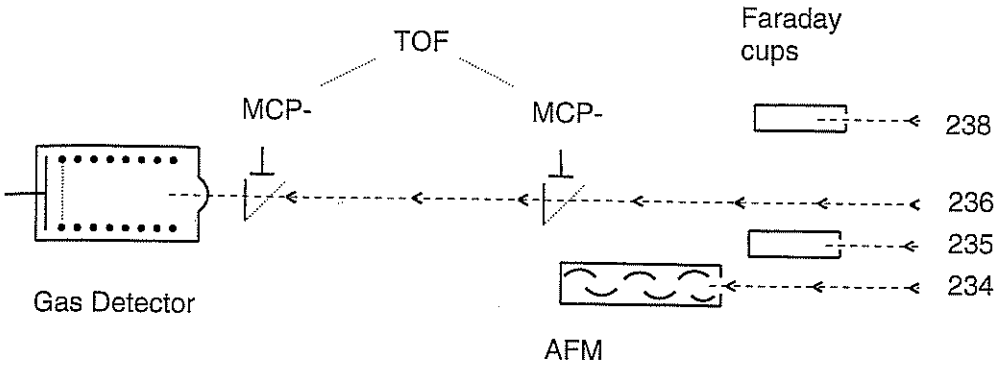

Fig. 7. Detector instrumentation at the focal plane of the high-energy actinide beam-line at ANSTO as in 2000. [Reprinted with permission from Hotchkis et al. (2000a).] Note that this has subsequently evolved.

et al., 2002). The yield for stripping $^{238}U^{16}O^-$ to $^{238}U^{5+}$ was measured to be 6%. A high-resolution 90° ESA after the analyzing magnet strongly suppresses ions with different M/q ratios. Any residual background ions are identified by a TOF system consisting of two micro-channel plate detectors. This is backed by an ionization chamber to discriminate against lower charge state ions of the same M/q. The overall efficiency of the detection system is 20–30%.

A slow-cycling procedure is employed for plutonium analyses. Switching times between isotopes are 15 s and measurement times range between 20 and 100 s (Hrnecek et al., 2005; Winkler et al., 2004). For ^{236}U, a quasi-fast switching procedure has been adopted. Ion source fluctuations are monitored by fast switching of the $^{238}U^{16}O^-$ beam into the low-energy off-axis Faraday cup during post-acceleration measurement of both the ^{238}U beam current and ^{236}U ions. Due to the small fractional mass difference between ^{238}U and ^{236}U, it is, however, necessary to change the accelerator voltage when switching between isotopes at the high-energy side. This takes ~15 s. Hence, the $^{238}U^{5+}$ beam current is measured only every 5 min. This frequency is quite adequate to monitor drifts in stripping yield (Steier et al., 2002; Vockenhuber et al., 2003).

6.5. *Munich*

The Munich facility is blessed with a very large analyzing magnet with a mass–energy product of 350 MeV-amu. This makes the use of foil stripping at a higher terminal voltage a viable option. An accelerating voltage of 12.5 MV is employed, and the 11^+ charge state selected. Ions are detected by a TOF system consisting of a MCP "start" detector and a "stop" detector which combines an ionization chamber to provide a ΔE signal and a silicon detector to provide both the timing signal and a residual-energy signal. Details may be found in Wallner et al. (2000).

6.6. *ETH, Zurich*

At Zurich, it has been shown that AMS of plutonium can be performed almost equally well on a small accelerator operating at only 0.3 MV (Fifield et al., 2004; Wacker et al., 2005). The

Table 2
Relative negative-ion formation probabilities for oxide ions of the actinides, normalized to Pu

Negative ion	Relative formation probability[a]
ThO^-	0.15 ± 0.01
UO^-	0.43 ± 0.04
NpO^-	0.77 ± 0.02
PuO^-	1.00

[a]Absolute negative ion yields can be derived from this table using the observation that the yield for uranium oxide is 0.3%.

1.2 MeV Pu ions are analyzed by a combination of 90° magnetic and electric analyzers, and detected in a gas ionization detector with a 40 or 50 nm thick silicon nitride window. Since the Pu ions lose only 300–400 keV in this window, the resolution of the detector is substantially better than a silicon detector, and is sufficient to resolve the 3^+ Pu ions from 2^+ and 1^+ ions with the same M/q, as shown in Figure 3. It appears that this system may even be suitable for high-sensitivity ^{236}U measurements (Wacker et al., 2005).

Perhaps paradoxically, this small system has the highest transmission of any AMS system for actinides. Stripping yield to the 3^+ charge state is surprisingly high at 20% and this, combined with minimal losses after stripping allow the Zurich system to achieve transmission as high as 15% from ion source to detector. By contrast, the corresponding figure for systems using the 5^+ charge state is ~3%.

6.7. *Weizmann Institute*

Techniques for analyzing both ^{236}U and plutonium isotopes have been developed by Paul et al. at the 14UD accelerator of the Weizmann Institute (Berkovits et al., 2000; Paul et al., 2001, 2003). Foil stripping to the 9^+ or 11^+ charge state at a terminal voltage of 7.1 MV was employed. Transmission of 0.1–0.2% is significantly less than at facilities where gas stripping is used. The detection system provides both time-of-flight and energy information for each ion.

6.8. *New facilities*

New AMS facilities based on 3 and 1 MV tandems have recently been installed in Naples and Seville, respectively. In both cases, the injection and analyzing magnets have been specified with future actinide measurements in mind.

7. Efficiency

Efficiency is the product of negative ion yield and transmission. Negative ion yield has been measured to be 0.3% for uranium by monitoring the current of $^{238}U^{16}O^-$ ions from a sample containing a known amount of uranium as it was run to exhaustion (Fifield et al., 1996). Relative yields for Th, U, Np and Pu are listed in Table 2 and were determined using samples containing these elements in known proportions (Fifield et al., 1997).

Transmission from ion source to detector varies from system to system. At ANU, transmission in the 5^+ charge state is ~3%. From Table 2, the overall efficiency for detecting a uranium ion is $\sim 10^{-4}$. For Pu, it is about a factor of two higher. Since backgrounds are very low, a signal of 10 counts is readily observable. Hence, sensitivities of $\sim 10^5$ atoms of ^{236}U, ^{237}Np or Pu are achievable with AMS.

8. Backgrounds

8.1. *Plutonium*

Although AMS of plutonium has intrinsically very low background levels, ions other than those of interest are also detected. These fall into two categories:

1. Other 5^+ ions with very similar energies. Of these, the most serious is ^{238}U, although ^{235}U or ^{232}Th are also possibilities. After selection by the analyzing magnet, $^{238}U^{5+}$ and $^{239}Pu^{5+}$ differ in energy by only 0.4%. This is well below the 3% resolution of the ionization detector. Those laboratories with a high-resolution ESA may be able to prevent the ^{238}U ions from reaching the detector, but a Wien filter will not in general deflect the $^{238}U^{5+}$ ions sufficiently to allow the interception of all of the ^{238}U ions before the detector. Hence, it is important to understand the origin of the ^{238}U ions and the likely extent of the problem.

   Uranium-containing negative molecular ions of mass 255, of which the most important is $^{238}U^{17}O^-$, are injected into the accelerator along with the $^{239}Pu^{16}O^-$ ions. Similarly, $^{238}U^{18}O^-$ ions are injected with $^{240}Pu^{16}O^-$. After molecular dissociation and stripping in the high-voltage terminal and subsequent acceleration, $^{238}U^{5+}$ and $^{239}Pu^{5+}$ ions differ in momentum by 0.25%. These particular $^{238}U^{5+}$ ions are not a problem because they are readily eliminated by the analyzing magnet, which is typically operated at a resolution of 0.1% or better in momentum.

   The problematic $^{238}U^{5+}$ ions are rather those that have the same *momentum* as the $^{239}Pu^{5+}$ ions and that therefore pass around the analyzing magnet. To satisfy this condition, the $^{238}U^{5+}$ must gain an extra 0.4% of energy. Some of the ions that are stripped to 6^+ in the terminal can undergo charge-changing collisions and change to 5^+. If these collisions occur ~3% of the way down the high-energy tube, the ^{238}U ions will have the correct energy to pass around the analyzing magnet. The probability of this process is critically dependent on the vacuum in the high-energy tube—the better the vacuum, the lower the probability. Since gas-stripping is employed, a recirculating gas stripper with additional differential pumping to minimize the gas entering the high-energy tube is crucial. Child et al. (2005) have explored this ^{238}U background as a function of the amount of uranium added to a blank sample, and found that even 1 ng of uranium (i.e. about 1 ppm in a 1 mg sample) leads to an apparent ^{239}Pu signal of 10 fg. A sample to which no uranium was added yielded an apparent ^{239}Pu signal of ~3 fg due to residual uranium in the ion source or intrinsic to the sample. Their results are shown in Figure 8. A similar (unpublished) study performed at the ANU showed a sensitivity to uranium concentration that was two orders of magnitude lower than reported by Child et al. (2005), i.e. 100 ng of uranium was

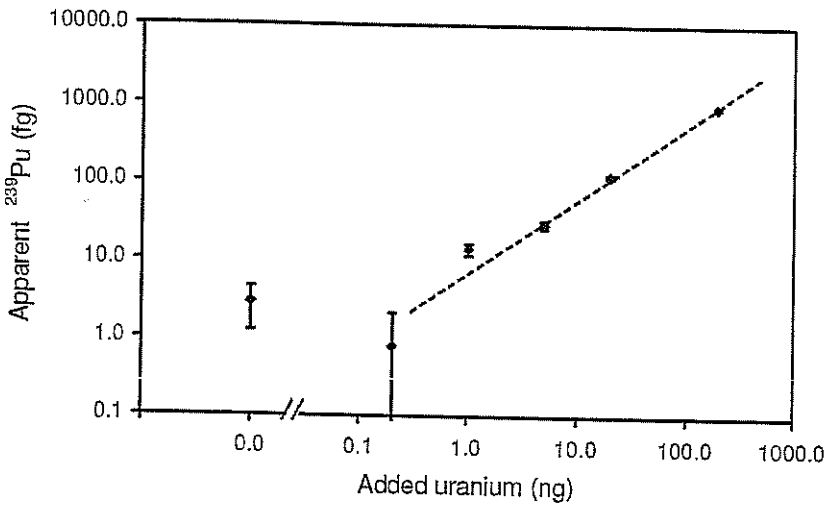

Fig. 8. Apparent Pu in fg due to background ^{238}U ions that are indistinguishable from ^{239}Pu ions in the detector, as a function of uranium concentration in the sample. [Reprinted with permission from Child et al. (2005).]

required to produce an apparent ^{239}Pu signal of 10 fg. This is borne out by regular measurements at the ANU on process blanks which routinely exhibit an apparent ^{239}Pu signal of <0.2 fg. This lower sensitivity to uranium highlights the importance of the vacuum in the high-energy acceleration tube close to the high-voltage terminal. In the ANU's 14UD accelerator, this is typically better than 10^{-8} Torr due to the excellent pumping of the gas stripper and the intrinsically high vacuum of the NEC tube design.

Uranium backgrounds at ^{240}Pu can be higher than at ^{239}Pu because the $^{238}U^{18}O^{-}$ ion is five times more prolific than the $^{238}U^{17}O^{-}$ ion. If these oxide molecules, rather than the $^{238}U^{16}OH^{-}$ ion or the high-energy tail of the $^{238}U^{16}O^{-}$ ion distribution, are the principal source of ^{238}U ions in the accelerator, then the ^{238}U background at ^{240}Pu will be approximately five times higher than at ^{239}Pu. There is some evidence that this is the case, at least for the ANU system (Fifield et al., 1996).

2. The second category of non-Pu ions that may arrive at the detector is ions with lower charge states but approximately the same M/q. To consider a specific example, any $^{191}Pt^{4+}$ ions with the same ME/q^2 as $^{239}Pu^{5+}$ ions will be only slightly deflected by a Wien filter (or will pass around an ESA) and will therefore reach the ionization detector when the AMS system is set to transmit ^{239}Pu. Because they have only 4/5 of the energy of the ^{239}Pu ions, they are readily distinguished by the ionization chamber, and hence are only a problem if counting rates are high. They have their origin in injection of molecular negative ions of mass 255. Possibilities involving common elements would be $^{191}Pt^{16}O_4$, $^{191}Pt^{48}Ti^{16}O$, or $^{191}Pt^{32}S^{16}O_2$. Because M/q for $^{191}Pt^{4+}$ ions is not exactly the same as for $^{239}Pu^{5+}$ ions, a charge-changing collision from 5^+ to 4^+ in the high-energy tube is necessary to give the ^{191}Pt the correct energy to traverse the analyzing magnet. Taken together, the low natural abundance of platinum, the complexity of the molecules, and the low probability of the charge-changing collision result in extremely low counting rates of $^{191}Pt^{4+}$ ions at the detector. This is equally true of the lower charge state ions $^{143}Sm^{3+}$, $^{96}Mo^{2+}$ and $^{48}Ti^{+}$.

Counting rates of these background ions are therefore low, and typical spectra at the ^{239}Pu settings are very clean, as can be seen in Figure 2a. Similar considerations apply to ^{242}Pu, for which a typical spectrum is shown in Figure 2c.

The situation is, however, rather different for $^{240}Pu^{5+}$. In this case, M/q is an integer. Ignoring differences in binding energies for the moment, it follows that there is no need to invoke a charge-changing collision in the high-energy tube. Atoms stripped to $^{48}Ti^{+}$, $^{96}Mo^{2+}$, $^{144}Sm^{3+}$, and $^{192}Pt^{4+}$ in the gas stripper alone will have the correct energy to pass around the analyzing magnet. Hence, counting rates of these ions can be orders of magnitude higher at the ^{240}Pu settings than at ^{239}Pu or ^{242}Pu settings, as illustrated by Figure 2b. Nevertheless, counting rates are generally well within the capabilities of the detector. Note, however, that ^{240}Pu is rather less tightly bound than the lighter interferences, i.e. M/A for ^{240}Pu is 0.12% greater than ^{96}Mo for example. As a result, $^{240}Pu^{5+}$ and $^{96}Mo^{2+}$ do not follow exactly the same average trajectories in the analyzing magnet. With appropriate apertures, the counting rates of the M/q interferences can be reduced substantially, especially when the analyzing magnet is followed by a high-resolution ESA.

8.2. *Uranium-236*

AMS of ^{236}U must contend with the fact that uranium is a major constituent of the sample. Backgrounds from ^{238}U and ^{235}U, which arise in essentially the same way as the ^{238}U background in the plutonium case described above, will therefore be a more serious problem than was the case for plutonium.

At the ^{236}U settings, the mass-252 $^{236}U^{16}O^{-}$ ion is selected for injection into the accelerator. Other ions of the same mass, but with either ^{238}U or ^{235}U as a constituent, are $^{238}U^{14}N^{-}$, $^{238}U^{12}CH_2^{-}$, $^{235}U^{17}O^{-}$, and $^{235}U^{16}OH^{-}$. Of these, $^{235}U^{17}O^{-}$ is unavoidable and will be injected with a beam current of ~0.3 pA (~2×10^6 ions/s) when the $^{238}U^{16}O^{-}$ output is 100 nA. Experience with plutonium suggests that the $U^{16}OH^{-}$ beam is generally weaker than the $U^{17}O^{-}$ beam.

Measurements on test samples at the ANU showed that, although the $^{238}U^{14}N^{-}$ ion can be a significant source of background if the sample is in the form of uranium nitrate, the normal procedure of baking the samples at 800 °C is very effective at eliminating nitrogen. Hence the $^{238}U^{14}N^{-}$ ion does not contribute materially to the ^{238}U background for "real" samples.

Further, the addition of 1 mg of graphite to a uranium oxide sample did not increase the ^{238}U background, which implies that the $^{238}U^{12}CH_2^{-}$ ion is not an important source of background either.

In fact, the principal source of background appears to arise from the low-energy tail of the $^{238}U^{16}O^{-}$ beam. Specifically, if a $^{238}U^{16}O^{-}$ ion has 0.8% less energy than normal, it will be accepted by the injector magnet and injected into the accelerator. The most likely mechanism for producing such lower-energy ions is the formation of "hot" molecules which break up during the extraction process in the ion source (Litherland, 1987). Similarly, $^{235}U^{16}O^{-}$ ions with 0.4% more energy than normal will also be accepted. Some ions can gain extra energy from the backscattered Cs ions during the sputtering process. A detailed discussion of the various mechanisms is given by Litherland (1987) in the context of carbon beams. Although the relative contributions of the different sources of background are difficult to quantify, it is

believed that these energy-degraded $^{238}U^{16}O^-$ ions are the dominant source of background in the ANU system.

Some AMS systems have an energy-analyzing ESA between the ion source and the injector magnet. Provided that this has sufficiently high resolution, the energy-degraded $^{238}U^{16}O^-$ or energy-enhanced $^{235}U^{16}O^-$ ions can be eliminated before the injector magnet. A resolution $E/\Delta E > 250$ would be required to eliminate both the $^{238}U^{16}O^-$ and $^{235}U^{16}O^-$ ions.

9. Sample preparation

Sample preparation methods have been adapted from techniques developed for alpha-particle counting. We shall briefly discuss only methods for plutonium. There are three stages:

(i) Initial scavenging of the plutonium from the original sample. If a ^{242}Pu spike is required, it is added at this stage. Four possibilities can be distinguished:
   (a) Soils and sediments. The plutonium will generally reside on the surfaces of the grains, and hence can be liberated by leaching in hot 8M nitric acid (Tims et al., 2004).
   (b) Water, including ice. Plutonium is co-precipitated with either $Fe(OH)_3$ or MnO_2 by adding a suitable amount of Fe or Mn and then making the solution alkaline with NaOH.
   (c) Biological samples, e.g., blood, faeces or urine. The Pu is generally co-precipitated with either calcium phosphate or calcium/magnesium phosphate.
   (d) Rocks, and in particular uranium ores (for measurement of Pu produced *in situ* by neutron absorption by ^{238}U). After crushing and sieving, the <250 μm fraction is dissolved in a 40:60 mixture of concentrated HF and HNO_3. This effectively dissolves any uranium-bearing minerals, including silicates. Often, a residue of graphite and sulfides remains after dissolution, but these contain very little of the uranium, or by implication, of the plutonium. Insoluble fluorides are also precipitated. Since PuF_4 is insoluble, it is necessary to take the fluorides back into solution with HNO_3 and to drive off the fluorine as HF by repeatedly drying down from nitric acid solution.

(ii) Separation of the actinides from everything else. After taking the scavenged sample back into solution, this separation is usually accomplished with U-TEVA™ (uranium tetravalent) ion-exchange resin (Eichrom Industries, Chicago). The sample is loaded on to the column in 3M nitric acid, and only uranium and other tetravalent actinides are retained on the column as nitrate complexes. Plutonium and thorium can then be selectively eluted by a mixture of 5M hydrochloric and 0.05M oxalic acids. Uranium is subsequently eluted with dilute 0.01M hydrochloric acid.

(iii) Plutonium may be separated from any residual uranium, and less importantly from thorium and other actinides, on an anion-exchange column, Bio-Rad AG 1-X8 for example. The plutonium is loaded on to the column in 8M nitric acid and any residual uranium washed through with additional acid. Thorium can then be eluted with 12M hydrochloric acid. Finally, plutonium is eluted from the resin with a freshly made, warm (40 °C) mixture of 12M HCl and 0.1M NH_4I. The iodide ion reduces Pu to its trivalent state, breaking the anionic complex and releasing the Pu from the column.

At the end of this procedure, the plutonium and very little else is in solution. In order to produce a sample for the ion source, considerably more bulk than would be provided by a few pg of Pu is, however, required. Almost invariably, this has been provided by iron oxide. Typically 1–2 mg of iron as $Fe(NO_3)_3$ is added to the plutonium-containing solution. The solution is then either simply evaporated to dryness, or iron is precipitated as $Fe(OH)_3$ by making the solution alkaline. The resulting solid is converted to Fe_2O_3 by baking at 800 °C, mixed with a conductor that has variously been aluminum, silver, copper or niobium, and pressed into a sample holder.

In contrast to plutonium, where efficiency is paramount and where it is important to ensure valence equilibrium between the ^{242}Pu spike and Pu in the sample, the chemistry for extracting uranium is more forgiving in the sense that the principal requirement is only that enough uranium be extracted for a measurement, Since no spike is added, efficiency of extraction and equilibration are not serious issues.

10. Applications

10.1. *Tracing discharges from plutonium-processing and fuel reprocessing plants*

In a series of papers, Oughton and co-workers have employed AMS to measure plutonium concentrations and plutonium and uranium isotopic ratios in regions affected by the nuclear-weapons production complex of the former Soviet Union (Figure 9). Specifically

(i) In the vicinity of the Mayak production and processing facility in the Urals, significant releases of plutonium have contaminated the local environment. In the 1950's, waste containing weapons grade plutonium with low $^{240}Pu/^{239}Pu$ ratios (<5%) was released directly to the Techa River. The Techa is a tributary of the Ob river which is one of the two major rivers draining Siberia to the Arctic Ocean. Subsequently, containment dams were built to intercept waste, and the plant reprocessed an increasing proportion of waste from civil nuclear power reactors. Hence $^{240}Pu/^{239}Pu$ and $^{236}U/^{238}U$ ratios change over time. In addition, an explosion in a high-level waste tank in 1963 sent a plume of radioactive material to the northeast of the plant. Plutonium measurements have been carried out in the swamp just downstream of the containment dams, which would have received some of the earliest releases, in water and sediments from the dams themselves, in soils and sediments down the Techa River and from areas affected by the Khyshtym accident, and in present-day water from the river (Borretzen et al., 2005; Oughton et al., 2000). In addition, $^{236}U/^{238}U$ ratios have been measured in both the swamp and the dams (Borretzen et al., 2005). Taken together, these give a rather complete picture of the quantities and origins of plutonium in the environs of the plant, and the extent to which it has dispersed. In particular, plutonium from the plant's operations is barely detectable in the river at distances greater than 200 km from the plant.

(ii) In contrast, measurements in sediments and water from the other major Siberian river, the Yenisey, point to an influence of the Krasnoyarsk processing plant. Located 1000 km upstream from the estuary, its influence is evidenced by low $^{240}Pu/^{239}Pu$ ratios in both water and sediment from the upper reaches of the estuary (Lind et al., 2006; Skipperud

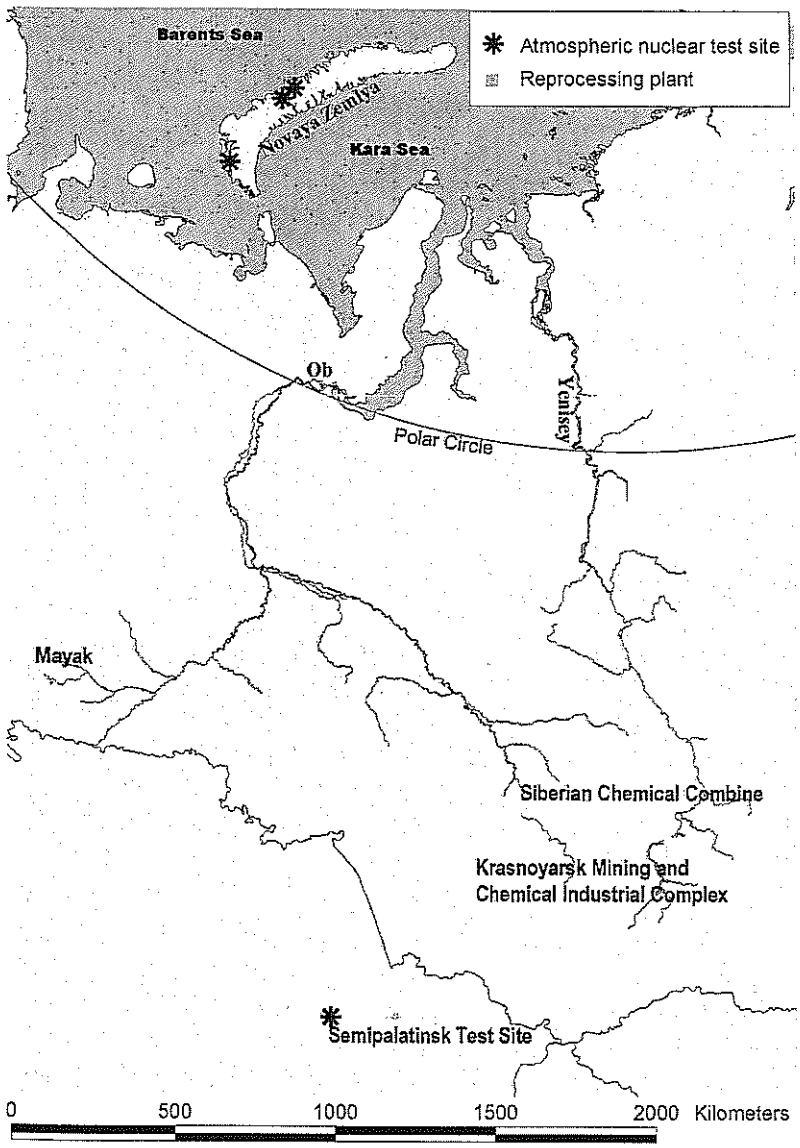

Fig. 9. Map of the Ob and Yenisey rivers showing sources of weapons' related contamination. The squares represent plutonium production and reprocessing facilities, and the stars nuclear weapon test sites. [From Skipperud et al. (2004).]

et al., 2004). This influence extends out into the Kara Sea, and back into the adjacent estuary of the Ob River.

(iii) Dumping of nuclear reactors from decommissioned submarines and other nuclear waste has occurred near Novaya Zemlya in the Russian Arctic. Ratios of $^{240}Pu/^{239}Pu$ have been employed to monitor possible leakage from these dumping sites (Oughton et al., 2004).

AMS has also been employed to study the dispersal of ^{237}Np and ^{236}U discharged from the Sellafield reprocessing plant in Cumbria, UK. Keith-Roach et al. (2000) measured the seasonal variation of ^{237}Np in pore water in a nearby salt marsh, and compared it with Pu and ^{241}Am in order to investigate the influence of microbial activity in mobilizing these isotopes. Marsden et al. (2001, 2006) measured ^{236}U/^{238}U ratios as a function of depth in sediments from the same marsh to complement radiometric measurements of concentrations of Pu isotopes, ^{241}Am and ^{244}Cm. Comparison with the documented history of releases from the Sellafield plant yields important information on the mechanisms that disperse the discharges into the environment.

10.2. *Human biochemistry of plutonium*

A major benefit of the high sensitivity of AMS is that it allows biomedical studies on *human* subjects because doses of long-lived radionuclides can be kept very low. Plutonium is a particular case in point, since its isotopes are α-particle emitters and the element is chemically toxic. Nature has been kind in that the longest-lived plutonium isotope, ^{244}Pu, has a half-life of 80 Ma and hence a very low specific activity. Further, although it can be extracted from spent reactor fuel, it was produced in only negligible quantities by nuclear weapons testing. Hence, the combination of low specific activity and absence from the natural environment make it a useful tracer of plutonium uptake, retention and excretion in human subjects. Two studies in which AMS has been used to detect the ^{244}Pu in blood, urine and fecal samples have been reported (Etherington et al., 2003; Newton et al., 2005; Stradling et al., 2002).

In the first (Newton et al., 2005), a group of six women were given a dose of mixed ^{237}Pu and ^{244}Pu by intravenous injection in 1995. It was necessary to purify the ^{244}Pu by mass-separation so that only traces of the other plutonium isotopes remained, in order to minimize the radiological burden to the subjects. The ^{237}Pu, with its half-life of 37 days, allowed the short term behavior of the dose to be followed by γ-ray counting of the 100 keV X-rays that are emitted following its β-decay to ^{237}Np. Subsequently, it has been possible to follow the decline in plutonium in the subjects out to 8 years by measuring ^{244}Pu in blood and urine samples by AMS. Even after 8 years, ^{244}Pu is still detectable in a 20 ml blood sample. Results are shown in Figure 10, where they are compared with an extensively modified revision (Leggett et al., 2005) of the ICRP's current biokinetic model for systemic plutonium (ICRP, 1993).

The second study determined the uptake of plutonium from the lungs when the plutonium was attached to aerosols (Etherington et al., 2003; Stradling et al., 2002). This was designed to mimic the most probable pathway for uptake by workers in nuclear processing plants.

10.3. *Safeguards*

A potential application of AMS in the nuclear safeguards area is the identification of clandestine nuclear activities by measuring ^{236}U in small particles. These may have been collected as aerosols or from the leaves of plants, and elevated ^{236}U/^{238}U ratios would constitute unambiguous evidence of material that had passed through a nuclear reactor (Hotchkis et al., 2000a, 2000b).

A closely related application is the identification of areas contaminated by depleted uranium weaponry. Armour-piercing shells made of depleted uranium were used in the recent Iraq and

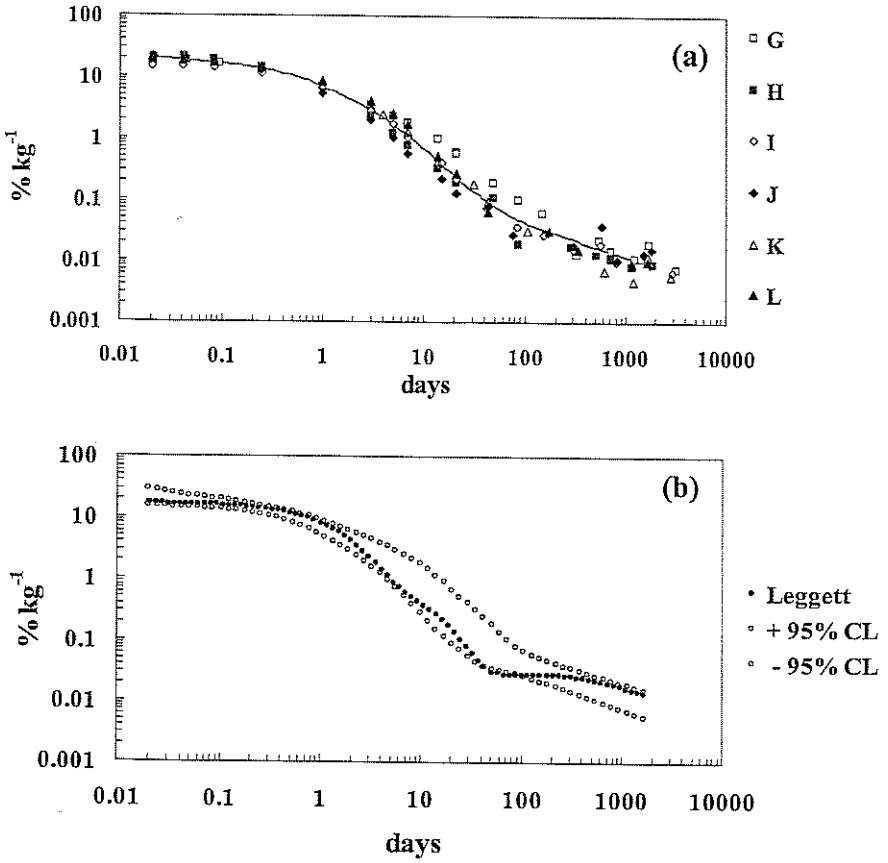

Fig. 10. (a) Concentrations (% of injection kg^{-1}) of plutonium in whole blood from six human female subjects as a function of time after injection with a mix of ^{237}Pu and ^{244}Pu. The line indicates the central tendency of the data. Data out to 60 days were obtained from γ-ray counting of ^{237}Pu decays. Subsequent data points, which extend out to 8 years after injection, were derived from AMS measurements of ^{244}Pu. (b) Concentrations from a revised version (Leggett et al., 2005) of the ICRP's current biokinetic model for systemic plutonium (ICRP, 1993), compared with the estimated ±95% range in adult females. [From Newton et al. (2005).]

Kosovo wars, and there are concerns about possible health effects on both military personnel and the civilian population of the affected areas. Depleted uranium is a by-product of the uranium-enrichment process, and the feedstock often contains some recycled reactor fuel with high levels of ^{236}U. Hence, some ^{236}U finds its way into the depleted uranium and can serve as a very sensitive fingerprint of the presence of depleted uranium in an area (Danesi et al., 2003). Again, the high sensitivity of AMS is required for its detection.

10.4. *Plutonium as a tracer of soil erosion and sediment transport*

Plutonium has advantages in terms of sample size, sensitivity and precision over the widely used ^{137}Cs as a tracer of soil erosion and sediment transport over the past 50 years. Both were

produced by nuclear weapons testing in the 1950s and 60s, and subsequently dispersed globally. Both bind tightly to soil and sediment particles, especially in terrestrial environments, and hence may be used to track the erosion of soil particles and their subsequent transport by river systems to the sea.

Approximately 5 times as many atoms of Pu as of ^{137}Cs were produced. Decay of ^{137}Cs in the intervening ~45 years has increased this ratio to ~14. In addition, there is some evidence that, in contrast to Pu, Cs desorbs from sediments in a saline environment. Whereas ^{137}Cs is readily detected via the 662 keV γ-ray emitted following its β-decay to ^{137}Ba, AMS is the method of choice for the detection of Pu in sediments, although some work has been done with α-particle counting. Sample sizes for AMS are typically 4 g of soil or sediment, and the same number of counts can be achieved for ^{239}Pu in 7 min of counting as is achieved for ^{137}Cs in 2 days of counting of a 100 g sample. Further, since the ^{137}Cs γ-ray peak sits on a background which must be subtracted, the statistical precision of the essentially background-free Pu measurements is higher. AMS counting times of ~1 h are quite feasible, which allows even higher precision to be achieved if desired. Sample preparation is somewhat more complex for Pu than for ^{137}Cs, but is not especially difficult. Surface-bound plutonium is leached from the grains with hot 8M nitric acid, and the Pu is subsequently separated from uranium and other elements on an anion-exchange column and then dispersed in Fe_2O_3 as described above. A spike of typically 4 pg of ^{242}Pu is added before leaching for normalization purposes.

A pilot study is underway in the 10,000 km^2 Herbert River catchment in NE Queensland, Australia to determine the relative merits of Pu and ^{137}Cs. This catchment covers grazing land in its upper reaches, undisturbed forest in the middle reaches, and intensive sugar-cane agriculture on the coastal plains. Soils and sediments collected from each of these land-use types show a very good correlation between Pu and ^{137}Cs, as shown in Figure 11.

10.5. *Ores*

Although ^{239}Pu and ^{236}U are generally thought of as exclusively man-made isotopes, they do in fact occur naturally in uranium ores, albeit at very low levels. Indeed, Seborg first reported the detection of natural plutonium in an ore from Cigar Lake in Saskatchewan as early as 1948. The processes that produce these isotopes are the same as in a reactor, i.e. neutron capture by ^{238}U and ^{235}U, respectively. The neutrons are generated principally by spontaneous fission of ^{238}U and by (α, n) reactions on light elements such as Na, Mg and Al. In a typical ore-bearing rock, these two contributions are approximately equal.

Potential applications include neutron flux monitoring (Purser et al., 1996), fingerprinting individual ores, and exploration for new uranium deposits. Neutron fluxes in an ore body are determined not only by the uranium content, but also by the water content, the concentrations of major neutron-producing elements such as Na, Mg and Al, and by the concentrations of trace neutron absorbers such as B, Gd and Sm. Since ^{239}Pu is produced by absorption of epithermal neutrons, whereas ^{236}U is produced largely by capture of thermal neutrons, it is possible to deduce both the thermal and epithermal neutron fluxes in the ore over the past 50 ka.

A particular concern of uranium-producing countries is that their uranium might find its way into nuclear weapons. Hence a fingerprint of a particular ore-body, or even of a particular

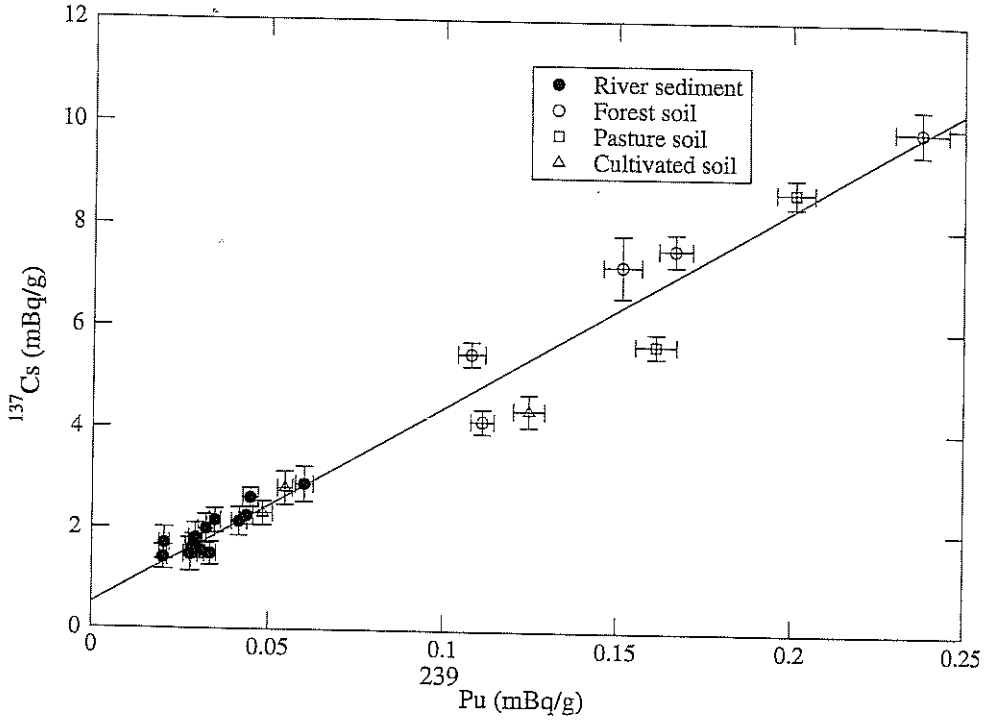

Fig. 11. Plot of ^{137}Cs concentration vs ^{239}Pu concentration for terrestrial samples from a range of land-use areas in the Herbert river catchment, N. Queensland, Australia. [From Everett et al. (2007).]

shipment of ore, would allow that specific uranium to be tracked. Any processing of the ore is not going to change the uranium isotopic composition, and hence the $^{236}U/^{238}U$ ratio might serve as such a fingerprint.

The presence of detectable amounts of ^{236}U in high-uranium groundwater would be a strong indicator that the uranium was derived from an ore-body. Hence, the $^{236}U/^{238}U$ ratio may prove to be a useful exploration tool in the search for new uranium deposits.

11. Summary

Accelerator mass spectrometry is proving to be an exquisitely sensitive tool for studying long-lived actinides in the environment, and an increasing number of AMS laboratories are adding an actinide capability to their repertoire. Applications range across a broad spectrum. Isotopes of plutonium are finding application in tracing the dispersal of releases from nuclear accidents and reprocessing operations, in studies of the biokinetics of the element in humans, and as a tracer of soil loss and sediment transport. Uranium-236 has also been used to track nuclear releases, but also has a role to play in nuclear safeguards and in determining the extent of environmental contamination in modern theaters of war due to the use of depleted uranium weaponry.

References

Bergquist, B.A., Marchetti, A.A., Martinelli, R.E., McAninch, J.E., Nimz, G.J., Proctor, I.D., Southon, J.R., Vogel, J.S. (2000). Technetium measurements by accelerator mass spectrometry at LLNL. *Nucl. Instrum. Methods B* **172**, 328–332.

Berkovits, D., Feldstein, H., Ghelberg, S., Hershkowitz, A., Navon, E., Paul, M. (2000). ^{236}U in uranium minerals and standards. *Nucl. Instrum. Methods B* **172**, 372–376.

Borretzen, P., Standring, W.J.F., Oughton, D.H., Dowdall, M., Fifield, L.K. (2005). Plutonium and uranium atom ratios and concentration factors in Reservoir 11 and Asanov Swamp, Mayak PA: An application of accelerator mass spectrometry. *Environ. Sci. Technol.* **39**, 92–97.

Brown, T.A., Marchetti, A.A., Martinelli, R.E., Cox, C.C., Knezovich, J.P., Hamilton, T.F. (2004). Actinide measurements by accelerator mass spectrometry at Lawrence Livermore National Laboratory. *Nucl. Instrum. Methods B* **223–224**, 788–795.

Child, D.P., Hotchkis, M.A.C., Williams, M.L. (2005). Improvements in actinide and fission product analysis by AMS—Raising the bar and lowering detection limits in heavy element AMS. In: Proceedings of the 46th Annual Meeting of the Institute for Nuclear Materials Management, Arizona, USA, July 10–14, 2005.

Danesi, P.R., Bleise, A., Burkart, W., Cabianca, T., Campbell, M.J., Makarewicz, M., Moreno, J., Tuniz, C., Hotchkis, M. (2003). Isotopic composition and origin of uranium and plutonium in selected soil samples collected in Kosovo. *J. Environ. Radioact.* **64**, 121–131.

Desideri, D., Meli, M.A., Roselli, C., Testa, C., Boulyga, S.F., Becker, J.S. (2002). Determination of ^{236}U and transuranium elements in depleted uranium ammunition by α-spectrometry and ICP-MS. *Anal. Bioanal. Chem.* **374**, 1091–1095.

Etherington, G., Stradling, G.N., Hodgson, A., Fifield, L.K. (2003). Anomalously high excretion of Pu in urine following inhalation of plutonium nitrate. *Radiat. Protect. Dosim.* **105**, 321–324.

Everett, S.J., Tims, S.G., Hancock, G.J., Fifield, L.K. (2007). Comparison of Pu and ^{137}Cs as tracers of sediment transport in terrestrial environments. *J. Environ. Radioact.*, submitted for publication.

Fehn, U., Snyder, G.T. (2005). Residence times and source ages of deep crustal fluids: interpretation of ^{129}I and ^{36}Cl results from the KTB-VB drill site, Germany. *Geofluids* **5**, 42–51.

Fehn, U., Snyder, G., Egeberg, P.K. (2000). Dating of pore waters with ^{129}I: Relevance for the origin of marine gas hydrates. *Science* **289**, 2332–2335.

Fehn, U., Snyder, G.T., Matsumoto, R., Muramatsu, Y., Tomaru, H. (2003). Iodine dating of pore waters associated with gas hydrates in the Nankai area, Japan. *Geology* **31**, 521–524.

Fifield, L.K. (1999). Accelerator mass spectrometry. *Rep. Prog. Phys.* **38**, 136–186.

Fifield, L.K., Cresswell, R.G., di Tada, M.L., Ophel, T.R., Day, J.P., Clacher, A.P., King, S.J., Priest, N.D. (1996). Accelerator mass spectrometry of plutonium isotopes. *Nucl. Instrum. Methods B* **117**, 295–303.

Fifield, L.K., Clacher, A.P., Morris, K., King, S.J., Cresswell, R.G., Day, J.P., Livens, F.R. (1997). Accelerator mass spectrometry of the planetary elements. *Nucl. Instrum. Methods B* **123**, 400–404.

Fifield, L.K., Carling, R.S., Cresswell, R.G., Hausladen, P.A., di Tada, M.L., Day, J.P. (2000). Accelerator mass spectrometry of ^{99}Tc. *Nucl. Instrum. Methods B* **168**, 427–436.

Fifield, L.K., Synal, H.-A., Suter, M. (2004). Accelerator mass spectrometry of plutonium at 300 kV. *Nucl. Instrum. Methods B* **223–224**, 802–806.

Gascard, J.C., Raisbeck, G., Sequeira, S., Yiou, F., Mork, K.A. (2004a). Correction to "The Norwegian Atlantic Current in the Lofoten basin inferred from hydrological and tracer data (I-129) and its interaction with the Norwegian Coastal Current". *Geophys. Res. Lett.* **31**, L08302.

Gascard, J.C., Raisbeck, G., Sequeira, S., Yiou, F., Mork, K.A. (2004b). The Norwegian Atlantic Current in the Lofoten basin inferred from hydrological and tracer data (I-129) and its interaction with the Norwegian Coastal Current. *Geophys. Res. Lett.* **31**, L01308.

Hotchkis, M., Fink, D., Tuniz, C., Vogt, S. (2000a). Accelerator mass spectrometry analyses of environmental radionuclides: sensitivity, precision and standardisation. *Appl. Radiat. Isotopes* **53** (1–2), 31–37.

Hotchkis, M.A.C., Child, D., Fink, D., Jacobsen, G.E., Lee, P.J., Mino, N., Smith, A.M., Tuniz, C. (2000b). Measurement of ^{236}U in environmental media. *Nucl. Instrum. Methods B* **172**, 659–665.

Hrnecek, E., Steier, P., Wallner, A. (2005). Determination of plutonium in environmental samples by AMS and alpha spectrometry. *Appl. Radiat. Isotopes* **63**, 633–638.

ICRP (1993). Age-dependent doses to members of the public from intake of radionuclides, Part 2: Ingestion dose coefficients. In: International Commission on Radiological Protection, Publication 67. *Ann. ICRP* **23** (3/4).

Keith-Roach, M.J., Day, J.P., Fifield, L.K., Bryan, N.D., Livens, F.R. (2000). Seasonal variations in interstitial water transuranium concentrations. *Environ. Sci. Technol.* **34**, 4273–4277.

Keith-Roach, M.J., Day, J.P., Fifield, L.K., Livens, F.R. (2001). Measurement of ^{237}Np in environmental water samples by accelerator mass spectrometry. *Analyst* **126**, 58–61.

Ketterer, M.E., Hafer, K.M., Link, C.L., Royden, C.S., Hartsock, W.J. (2003). Anthropogenic ^{236}U at Rocky Flats, Ashtabula River harbor, and Mersey estuary: three case studies by sector inductively coupled plasma mass spectrometry. *J. Environ. Radioact.* **67**, 191–206.

Kilius, L.R., Baba, N., Garwan, M.A., Litherland, A.E., Nadeau, M.-J., Rucklidge, J.C., Wilson, G.C., Zhao, X.-L. (1990). AMS of heavy ions with small accelerators. *Nucl. Instrum. Methods B* **52**, 357–365.

Kilius, L.R., Rucklidge, J.C., Soto, C. (1994). The dispersal of ^{129}I from the Columbia River estuary. *Nucl. Instrum. Methods B* **92**, 393–397.

Kraft, S., Adrianov, V., Bleile, A., Egelhof, P., Golser, R., Kiseleva, A., Kiselev, O., Kutschera, W., Meier, J.P., Priller, A., Shrivistava, A., Steier, P., Vockenhuber, C. (2004). First application of calorimetric low-temperature detectors in accelerator mass spectrometry. *Nucl. Instrum. Methods Phys. Res. A* **520**, 63–66.

Leggett, R.W., Eckerman, K.F., Khokhryakov, V.F., Suslova, K.G., Krahenbuhl, M.P., Millerc, S.C. (2005). Mayak worker study: An improved biokinetic model for reconstructing doses from internally deposited plutonium. *Radiat. Res.* **164**, 111–122.

Leonard, K.S., McCubbin, D., McDonald, P., Service, M., Bonfield, R., Conney, S. (2004). Accumulation of technetium-99 in the Irish Sea? *Sci. Total Environ.* **322**, 255–270.

Liechtenstein, V.K., Ivkova, T.M., Olshanski, E.D., Golser, R., Kutschera, W., Steier, P., Vockenhuber, C., Repnow, R., von Hahn, R., Friedrich, M., Kreissig, U. (2004). Recent investigations and applications of thin diamond-like carbon (DLC) foils. *Nucl. Instrum. Methods A* **521**, 197–202.

Lind, O.C., Oughton, D.H., Salbu, B., Skipperud, L., Sickel, M.A., Brown, E., Fifield, L.K., Tims, S.G. (2006). Transport of low ^{240}Pu/^{239}Pu atom ratio plutonium-species in the Ob and Yenisey Rivers to the Kara Sea. *Earth Planet. Sci. Lett.* **251**, 33–43.

Litherland, A.E. (1987). Fundamentals of accelerator mass spectrometry. *Philos. Trans. R. Soc. London A* **323**, 5–21.

Marsden, O.J., Livens, F.R., Day, J.P., Fifield, L.K., Goodal, P.S. (2001). Determination of U-236 in sediment samples by accelerator mass spectrometry. *Analyst* **126**, 633–636.

Marsden, O.J., Abrahamsen, L., Bryan, N.D., Day, J.P., Fifield, L.K., Gent, C., Goodal, P.S., Morris, K., Livens, F.R. (2006). Transport and accumulation of actinide elements in the near-shore environment: field and modelling studies. *Sedimentology* **53**, 237–248.

McAninch, J.E., Hamilton, T.F., Brown, T.A., Jokela, T.A., Knezovich, J.P., Ognibene, T.J., Proctor, I.D., Roberts, M.L., Sideras-Haddad, E., Southon, J.R., Vogel, J.S. (2000). Plutonium measurements by accelerator mass spectrometry at LLNL. *Nucl. Instrum. Methods B* **172**, 711–716.

McCartney, M., Rajendran, K., Olive, V., Busby, R.G., McDonald, P. (1999). Development of a novel method for the determination of ^{99}Tc in environmental samples by ICP-MS. *J. Anal. At. Spectrom.* **14**, 1849–1852.

Mironov, V., Kudrjashov, V., Yiou, F., Raisbeck, G.M. (2002). Use of ^{129}I and ^{137}Cs in soils for the estimation of ^{131}I deposition in Belarus as a result of the Chernobyl accident. *J. Environ. Radioact.* **59**, 293–307.

Moran, J.E., Fehn, U., Hanor, J.S. (1995). Determination of source ages and migration patterns of brines from the U.S. Gulf Coast basin using ^{129}I. *Geochim. Cosmochim. Acta* **59**, 5055–5069.

Newton, D., Talbot, R.J., Pich, G.M., Fifield, L.K., Priest, N.D. (2005). Long-term behavior of injected plutonium in healthy women. In: Oeh, U., Roth, P., Paretzke, H.G. (Eds.), Proceedings of 9th International Conference on Health Effects of Incorporated Radionuclides, Neuherberg, Germany, Nov 29–Dec 1, 2004. Available at http://www.gsf.de/heir/ProceedingsHEIR2004_ebook.pdf, pp. 311–317.

O'Donnell, R.G., Mitchell, P.I., Priest, N.D., Strange, L., Fox, A., Henshaw, D.L., Long, S.C. (1997). Variations in the concentration of plutonium, strontium-90 and total alpha-emitters in human teeth collected within the British Isles. *Sci. Total Environ.* **201**, 235–243.

Oughton, D.H., Fifield, L.K., Day, J.P., Cresswell, R.G., Skipperud, L., Di Tada, M.L., Salbu, B., Strand, P., Drozcho, E., Mokrov, Y. (2000). Plutonium from Mayak: Measurement of isotope ratios and activities using accelerator mass spectrometry. *Environ. Sci. Technol.* **34**, 1938–1945.

Oughton, D.H., Skipperud, L., Fifield, L.K., Cresswell, R.G., Salbu, B., Day, P. (2004). Accelerator mass spectrometry measurement of ^{240}Pu/^{239}Pu isotope ratios in Novaya Zemlya and Kara Sea sediments. *Appl. Radiat. Isotopes* **61**, 249–253.

Paul, M., Valenta, A., Ahmad, I., Berkovits, D., Bordeanu, C., Ghelberg, S., Hashimoto, Y., Hershkowitz, A., Jiang, S., Nakanishi, T., Sakamoto, K. (2001). Experimental limit to interstellar ^{244}Pu abundance. *Astrophys. J.* **558**, L133–L135.

Paul, M., Valenta, A., Ahmad, I., Berkovits, D., Bordeanu, C., Ghelberg, S., Hershkowitz, Y.H., Jiang, S., Nakanishi, T., Sakamoto, K. (2003). A window on nucleosynthesis through detection of short-lived radionuclides. *Nucl. Phys. A* **719**, C29–C39.

Purser, K.H., Kilius, L.R., Litherland, A.E., Zhao, X.-L. (1996). Detection of ^{236}U: a possible 100-million year neutron flux integrator. *Nucl. Instrum. Methods B* **113**, 445–452.

Raisbeck, G.M., Yiou, F. (1999). ^{129}I in the oceans: origins and applications. *Sci. Total Environ.* **238**, 31–41.

Raisbeck, G.M., Yiou, F., Zhou, Z.Q., Kilius, L.R. (1995). ^{129}I from nuclear fuel reprocessing facilities at Sellafield (U.K.) and La Hague (France); potential as an oceanographic tracer. *J. Mar. Syst.* **6**, 561–570.

Richter, S., Alonso, A., Bolle, W.D., Wellum, R., Taylor, P.D.P. (1999). Isotopic "fingerprints" for natural uranium ore samples. *Int. J. Mass Spectrom.* **193**, 9–14.

Rucklidge, J., Kilius, L., Fuge, R. (1994). ^{129}I in moss down-wind from the Sellafield nuclear fuel reprocessing plant. *Nucl. Instrum. Methods B* **92**, 417–420.

Skipperud, L., Oughton, D.H., Fifield, L.K., Lind, O.C., Tims, S., Brown, J., Sickel, M. (2004). Plutonium isotope ratios in the Yenisey and Ob estuaries. *Appl. Radiat. Isotopes* **60**, 589–593.

Snyder, G.T., Fehn, U. (2002). Origin of iodine in volcanic fluids: ^{129}I results from the Central American Volcanic Arc. *Geochim. Cosmochim. Acta* **66**, 3827–3838.

Snyder, G., Fehn, U. (2004). Global distribution of ^{129}I in rivers and lakes: implications for iodine cycling in surface reservoirs. *Nucl. Instrum. Methods Phys. Res. B* **223–224**, 579–586.

Snyder, G.T., Riese, W.C., Franks, S., Fehn, U., Pelzmann, W.L., Gorody, A.W., Moran, J.E. (2003). Origin and history of waters associated with coalbed methane: ^{129}I, ^{36}Cl, and stable isotope results from the Fruitland Formation, CO and NM. *Geochim. Cosmochim. Acta* **67**, 4529–4544.

Steier, P., Golser, R., Kutschera, W., Liechtenstien, V., Priller, A., Valenta, A., Vockenhuber, C. (2002). Heavy ion AMS with a "small" accelerator. *Nucl. Instrum. Methods B* **188**, 283–287.

Stradling, N., Etherington, G., Hodgson, A., Bailey, M.R., Hodgson, S., Pellow, P., Shutt, A.L., Birchall, A., Rance, E., Newton, D., Fifield, K. (2002). Comparison between biokinetics of inhaled plutonium nitrate and gadolinium oxide in humans and animals. *J. Radioanal. Nucl. Chem.* **252**, 315–325.

Suter, M., Döbeli, M., Grajcar, M., Müller, A., Stocker, M., Sun, G., Synal, H.-A., Wacker, L. (2007). Advances in particle identification in AMS at low energies. *Nucl. Instrum. Methods B* **259**, 165–172.

Tims, S.G., Hancock, G.J., Wacker, L., Fifield, L.K. (2004). Measurements of Pu and Ra isotopes in soils and sediments by AMS. *Nucl. Instrum. Methods B* **223–224**, 796–801.

Vockenhuber, C., Ahmad, I., Golser, R., Kutschera, W., Liechtenstein, V., Priller, A., Steier, P., Winkler, S. (2003). Accelerator mass spectrometry of heavy long-lived radionuclides. *Int. J. Mass Spectrom.* **223–224**, 713–732.

Wacker, L., Chamizo, E., Fifield, L.K., Stocker, M., Suter, M., Synal, H.A. (2005). Measurement of actinides on a compact AMS system working at 300 kV. *Nucl. Instrum. Methods B* **240**, 452–457.

Wallner, C., Faestermann, T., Gerstmann, U., Hillebrandt, W., Knie, K., Korschinek, G., Lierse, C., Pomar, C., Rugel, G. (2000). Development of a very sensitive AMS method for the detection of supernova-produced long living actinide nuclei in terrestrial archives. *Nucl. Instrum. Methods B* **172**, 333–337.

Winkler, S., Ahmad, I., Golser, R., Kutschera, W., Orlandini, K.A., Paul, M., Priller, A., Steier, P., Valenta, A., Vockenhuber, C. (2004). Developing a detection method of environmental ^{244}Pu. *Nucl. Instrum. Methods B* **223–224**, 817–822.

Wyse, E.J., Lee, S.H., Rosa, J.L., Povinec, P., de Mora, S.J. (2001). ICP-sector field mass spectrometry analysis of plutonium isotopes: recognizing and resolving potential interferences. *J. Anal. At. Spectrom.* **16**, 1107–1111.

Yiou, F., Raisbeck, G.M., Zhou, Z.Q., Kilius, L.R. (1994). ^{129}I from nuclear fuel reprocessing; potential as an oceanographic tracer. *Nucl. Instrum. Methods B* **92**, 436–439.

Yiou, F., Raisbeck, G.M., Christensen, G.C., Holm, E. (2002). ^{129}I/^{127}I, ^{129}I/^{137}Cs and ^{129}I/^{99}Tc in the Norwegian coastal current from 1980 to 1998. *J. Environ. Radioact.* **60**, 61–71.

Yiou, F., Raisbeck, G., Imbaud, H. (2004). Extraction and AMS measurement of carrier free ^{129}I/^{127}I from seawater. *Nucl. Instrum. Methods B* **223–224**, 412–415.

Ziegler, J.F., Biersack, J.P. (2003). SRIM—The Stopping and Range of Ions in Matter. http://www.srim.org.